

Composition and Property Measurements for PHA Phase 2 Glasses

by

T. B. Edwards

Westinghouse Savannah River Company
Savannah River Site
Aiken, South Carolina 29808

J. R. Harbour

R. J. Workman

RECEIVED
FEB 08 2000
O S T S

DOE Contract No. DE-AC09-96SR18500

This paper was prepared in connection with work done under the above contract number with the U. S. Department of Energy. By acceptance of this paper, the publisher and/or recipient acknowledges the U. S. Government's right to retain a nonexclusive, royalty-free license in and to any copyright covering this paper, along with the right to reproduce and to authorize others to reproduce all or part of the copyrighted paper.

WSRC-TR-99-00290

Revision 0

**Keywords: Coupled Operations
DWPF, PCT, PCCS,
Liquidus Temperature,
Salt Disposition, Viscosity**

Retention Time: Permanent

COMPOSITION AND PROPERTY MEASUREMENTS FOR PHA PHASE 2 GLASSES (U)

T. B. Edwards
J. R. Harbour
R. J. Workman

Westinghouse Savannah River Company
Savannah River Technology Center
Aiken, SC 29808



SAVANNAH RIVER SITE

PREPARED FOR THE U.S. DEPARTMENT OF ENERGY UNDER CONTRACT NO. DE-AC09-96SR18500

DISCLAIMER

This report was prepared as an account of work sponsored by an agency of the United States Government. Neither the United States Government nor any agency thereof, nor any of their employees, makes any warranty, express or implied, or assumes any legal liability or responsibility for the accuracy, completeness, or usefulness of any information, apparatus, product, or process disclosed, or represents that its use would not infringe privately owned rights. Reference herein to any specific commercial product, process, or service by trade name, trademark, manufacturer, or otherwise does not necessarily constitute or imply its endorsement, recommendation, or favoring by the United States Government or any agency thereof. The views and opinions of authors expressed herein do not necessarily state or reflect those of the United States Government or any agency thereof.

This report has been reproduced directly from the best available copy.

Available to DOE and DOE contractors from the Office of Scientific and Technical Information, P.O. Box 62, Oak Ridge, TN 37831; prices available from (615) 576-8401.

Available to the public from the National Technical Information Service, U.S. Department of Commerce, 5285 Port Royal Road, Springfield, VA 22161.

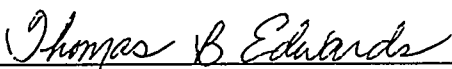
DISCLAIMER

Portions of this document may be illegible in electronic image products. Images are produced from the best available original document.

COMPOSITION AND PROPERTY MEASUREMENTS FOR PHA PHASE 2 GLASSES (U)

August 18, 1999

Document Approvals



T. B. Edwards, Author
Statistical Consulting Section

9/2/99

Date



J. R. Harbour, Author
Immobilization Technology Section

9/8/99

Date



R. J. Workman, Author
Immobilization Technology Section

9/8/99

Date



K. G. Brown, Technical Review
Immobilization Technology Section

9/2/99

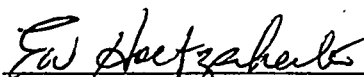
Date



R. C. Tuckfield, Manager
Statistical Consulting Section

9/8/99

Date



E. W. Holtzschner, Manager Immobilization Technology Section
Authorized Derivative Classifier

9-8-99

Date

This page intentionally left blank.

TABLE OF CONTENTS

Summary and Conclusions	1
Introduction	1
Results and Discussion	2
Chemical Compositions	2
PCT Results	7
Viscosity at 1150 °C	9
Liquidus Temperature (T _L)	10
Surface Crystallization	11
Phase Separation	11
Conclusions	12
References	13
Appendix: Supplemental Tables and Exhibits	15

This page intentionally left blank.

SUMMARY AND CONCLUSIONS

The results presented in this report are for six Phase 2 Precipitate Hydrolysis Aqueous (PHA) glasses, each of which was targeted to contain 30 wt% simulated PUREX sludge on an oxide basis. The target PHA concentration was varied from 7 to 10 to 13 wt % oxides both at 1.25 and 2.5 wt % oxides of washed monosodium titanate (MST). However, the PHA targets were not achieved.

The results of the chemical composition analyses of the PHA Phase 2 glasses revealed a significant problem with certain elements. Both boron and sodium were higher than the target values, whereas potassium and copper were less than the target values. This suggested a problem with batching of the PHA for this phase. An analysis of the data, in which several different scenarios were considered and then tested by calculation, revealed that the probable cause was the use of anhydrous sodium borate rather than the intended hydrated sodium borate. The measured values are both qualitatively and quantitatively consistent with this error.

A recovery from this error was made by rebatching and melting glasses pha14, pha15, pha17, and pha18. The results will be included in Phase 4, PHA report. It was decided to report the results for the current glasses, even though they missed the target, since they provide additional insight into the durability of the PHA glasses. The viscosity results provide evidence for the predictability of the viscosity model at these high PHA loadings that have very low viscosity values.

Only four of the six glasses were durable when compared to the EA (Environmental Assessment) glass (as determined by the 7-day Product Consistency Test, the PCT). Glasses pha15 and pha18, with the highest level of PHA, were not durable and were outside the limits of predictability. Both glasses leached less than EA but their measured compositions led to these glasses not falling within the acceptance region for durability as established by the Product Composition Control System (PCCS) used by the Defense Waste Processing Facility (DWPF). Although the PHA target was not achieved, a relatively small increase in boron and sodium over that targeted resulted in failure of the glasses from a PCT perspective. This result leads to a caution for all the results obtained from both variability studies (PHA and CST). The current studies selected fixed points in compositional space and did not permit variation in the compositions of each element independently. As one increases the variability of elements and fabricates and tests the resultant glasses, a threshold usually appears. Passing this threshold can lead to poor glass quality or unacceptable processing parameters. Thus, the size of the actual processing window is not revealed from this type of study. On the other hand, the inadvertent production of pha15 and pha18 glasses provides evidence that such a threshold does exist for these glasses.

All six glasses passed the homogeneity constraint indicating that amorphous phase separation should not be an issue. It is not clear what the mechanism is for the durability failure of glasses pha15 and pha18, but the homogeneity model used by PCCS to screen for phase separation, if correct, points to some other cause.

The models currently in PCCS were also used to calculate liquidus and viscosity for these six glasses. The viscosity model appears to work well at predicting the very low viscosities measured for these glasses. The viscosity values were either below or close to the lower limit of 20 poise for operation at DWPF. The viscosity model is not conservative to the lower limit (i.e., the predicted viscosities are not less than the measured viscosities). No crystallization was observed for these glasses even though the models predicted that the liquidus temperatures would be mostly unacceptable for these compositions.

INTRODUCTION

One of the Alternative Salt Disposition Flowsheets being considered would require that the Defense Waste Processing Facility (DWPF) vitrify a coupled feed containing high level waste (HLW) and Precipitate Hydrolysis Aqueous (PHA). A Technical Task Request (TTR) [1] was received by the

Savannah River Technology Center (SRTC) requesting that a glass variability study be conducted to explore the processability and product quality of the glass composition region for this alternative to the In-Tank Precipitation (ITP) Process. A Task Technical and Quality Assurance (TT&QA) plan [2] was issued by SRTC in response to the TTR. The objective of this task is to obtain information on the feasibility of incorporating anticipated levels of PHA into DWPF glass with and without doubling the nominal levels of monosodium titanate (MST).

A set of target compositions from which the glasses supporting this task are to be selected was provided in the memorandum appearing as Attachment I of the report of the PHA Phase 1 results [3]. Process and product property predictions for these glasses are also provided in that memorandum. The candidate glasses identified in that memorandum involved three sludge types: Purex, HM, and Blend; covered sludge loadings (in the glass) of 22, 26, and 30 oxide weight percent (wt%); utilized PHA loadings (in the glass) of 7, 10, and 13 oxide wt%; and included MST concentrations (in the glass) at 1.25 and 2.5 wt%. For each composition, the remainder of the glass consisted of Frit 202. The glasses, batched and fabricated using the Purex sludge at a target loading of 30 wt% of the glass, were selected to comprise Phase 2 of this study. The general, target compositions of these glasses are provided in Table 1.

Table 1: General Compositions of the PHA Phase 2 Glasses

Glass ID	Purex Sludge	PHA	MST	Frit
pha13	30%	7%	1.25%	61.75%
pha14	30%	10%	1.25%	58.75%
pha15	30%	13%	1.25%	55.75%
pha16	30%	7%	2.5%	60.50%
pha17	30%	10%	2.5%	57.50%
pha18	30%	13%	2.5%	54.50%

The properties of interest for these glasses included durability (as measured by the 7-day Product Consistency Test (PCT) [4]), viscosity at 1150 °C, and liquidus temperature. The purpose of this report is to provide and investigate comparisons between

- the measured and target compositions of this set of Phase 2 PHA glasses and
- the property measurements and their predictions.

The impact of these results on the path forward selected for this preliminary, PHA glass variability study will also be discussed.

RESULTS AND DISCUSSION

The six glasses comprising Phase 2 of the PHA study were designated as pha13 through pha18. Composition and property measurements of these glasses were conducted in parallel with the six glasses comprising Phase 2 of the other ITP replacement alternative, which is designated as the Crystalline Silicotitanate (CST) study. This helps ensure that the PHA and CST glasses are fabricated, characterized, and analyzed under very similar conditions. Included in the attachments of the CST Phase 2 report [5] are the analytical plans that were used to generate the measurements required to support both (CST and PHA) studies. These plans, which are identified in the discussion that follows, were prepared to support the overall Technical Task and QA plan [2] and the analytical study plan [6]. The results of these measurements (both composition and properties) are presented in this section.

Chemical Compositions

Table 2 provides the target oxide compositions for each of the PHA glasses. See Attachment I of [3] for details on the development of these target compositions. The Phase 2 glasses, as previously stated, appear as pha13 through pha18 in Table 2.

Table 2: Target Oxide Compositions (in weight percents, wt%'s) of the PHA Glasses

Sludge	MST	PHA	Frit 202	Glass												Na ₂ O
				ID	Al ₂ O ₃	B ₂ O ₃	BaO	CaO	Cr ₂ O ₃	CuO	Fe ₂ O ₃	K ₂ O	Li ₂ O	MgO	MnO	
22	1.250	7	69.750	pha01	2.540	7.974	0.084	0.945	0.106	0.568	9.899	3.350	4.785	1.448	1.727	7.869
22	1.250	10	66.750	pha02	2.522	8.803	0.084	0.941	0.106	0.791	9.897	4.730	4.579	1.389	1.727	8.017
22	1.250	13	63.750	pha03	2.504	9.632	0.084	0.936	0.106	1.014	9.894	6.110	4.373	1.329	1.727	8.165
22	2.500	7	68.500	pha04	2.532	7.876	0.084	0.943	0.106	0.568	9.898	3.350	4.699	1.423	1.727	7.944
22	2.500	10	65.500	pha05	2.514	8.705	0.084	0.939	0.106	0.791	9.896	4.730	4.493	1.364	1.727	8.092
22	2.500	13	62.500	pha06	2.496	9.534	0.084	0.934	0.106	1.014	9.893	6.110	4.288	1.304	1.727	8.240
26	1.250	7	65.750	pha07	2.901	7.660	0.099	1.092	0.125	0.576	11.685	3.365	4.510	1.381	2.041	8.116
26	1.250	10	62.750	pha08	2.883	8.488	0.099	1.088	0.125	0.800	11.683	4.745	4.305	1.322	2.041	8.264
26	1.250	13	59.750	pha09	2.865	9.317	0.099	1.083	0.125	1.023	11.681	6.125	4.099	1.262	2.041	8.412
26	2.500	7	64.500	pha10	2.894	7.561	0.099	1.090	0.125	0.576	11.684	3.365	4.425	1.356	2.041	8.191
26	2.500	10	61.500	pha11	2.876	8.390	0.099	1.086	0.125	0.800	11.682	4.745	4.219	1.297	2.041	8.339
26	2.500	13	58.500	pha12	2.858	9.219	0.099	1.081	0.125	1.023	11.680	6.125	4.013	1.237	2.041	8.487
30	1.250	7	61.750	pha13	3.263	7.345	0.114	1.239	0.144	0.585	13.472	3.380	4.236	1.314	2.355	8.363
30	1.250	10	58.750	pha14	3.245	8.174	0.114	1.234	0.144	0.808	13.470	4.760	4.030	1.255	2.355	8.511
30	1.250	13	55.750	pha15	3.227	9.003	0.114	1.230	0.144	1.031	13.467	6.140	3.824	1.195	2.355	8.659
30	2.500	7	60.500	pha16	3.256	7.246	0.114	1.237	0.144	0.585	13.471	3.379	4.150	1.289	2.355	8.438
30	2.500	10	57.500	pha17	3.238	8.075	0.114	1.233	0.144	0.808	13.469	4.759	3.945	1.230	2.355	8.586
30	2.500	13	54.500	pha18	3.220	8.904	0.114	1.228	0.144	1.031	13.466	6.139	3.739	1.170	2.355	8.734

Table 2: Target Oxide Composition (in weight percents, wt%'s) of the PHA Glasses (continued)

Sludge	MST	PHA	Frit 202	Glass												(SO ₄) ⁻
				ID	NiO	P ₂ O ₅	PbO	SiO ₂	TiO ₂	U ₃ O ₈	ZnO	ZrO ₂	F ⁻	Cl ⁻		
22	1.250	7	69.750	pha01	0.930	0.030	0.096	53.684	1.128	2.003	0.086	0.109	0.032	0.240	0.173	
22	1.250	10	66.750	pha02	0.930	0.030	0.096	51.404	1.127	2.003	0.086	0.109	0.032	0.240	0.173	
22	1.250	13	63.750	pha03	0.930	0.030	0.096	49.124	1.125	2.003	0.086	0.109	0.032	0.240	0.173	
22	2.500	7	68.500	pha04	0.930	0.030	0.096	52.734	2.226	2.003	0.086	0.109	0.032	0.240	0.173	
22	2.500	10	65.500	pha05	0.930	0.030	0.096	50.454	2.225	2.003	0.086	0.109	0.032	0.240	0.173	
22	2.500	13	62.500	pha06	0.930	0.030	0.096	48.174	2.224	2.003	0.086	0.109	0.032	0.240	0.173	
26	1.250	7	65.750	pha07	1.099	0.036	0.114	50.766	1.126	2.367	0.102	0.129	0.038	0.283	0.205	
26	1.250	10	62.750	pha08	1.099	0.036	0.114	48.486	1.125	2.367	0.102	0.129	0.038	0.283	0.205	
26	1.250	13	59.750	pha09	1.099	0.036	0.114	46.206	1.124	2.367	0.102	0.129	0.038	0.283	0.205	
26	2.500	7	64.500	pha10	1.099	0.036	0.114	49.816	2.224	2.367	0.102	0.129	0.038	0.283	0.205	
26	2.500	10	61.500	pha11	1.099	0.036	0.114	47.536	2.223	2.367	0.102	0.129	0.038	0.283	0.205	
26	2.500	13	58.500	pha12	1.099	0.036	0.114	45.256	2.222	2.367	0.102	0.129	0.038	0.283	0.205	
30	1.250	7	61.750	pha13	1.268	0.041	0.132	47.849	1.125	2.731	0.118	0.149	0.043	0.327	0.236	
30	1.250	10	58.750	pha14	1.268	0.041	0.132	45.569	1.123	2.731	0.118	0.149	0.043	0.327	0.236	
30	1.250	13	55.750	pha15	1.268	0.041	0.132	43.289	1.122	2.731	0.118	0.149	0.043	0.327	0.236	
30	2.500	7	60.500	pha16	1.268	0.041	0.132	46.899	2.223	2.731	0.118	0.149	0.043	0.327	0.236	
30	2.500	10	57.500	pha17	1.268	0.041	0.132	44.619	2.221	2.731	0.118	0.149	0.043	0.327	0.236	
30	2.500	13	54.500	pha18	1.268	0.041	0.132	42.339	2.220	2.731	0.118	0.149	0.043	0.327	0.236	

Predictions for the properties of interest generated for these target compositions by the models utilized by the Defense Waste Processing Facility (DWPF) are also included in the discussion provided in Attachment I of [3]. These properties, for a given composition, relate to its processability and its product quality. For a given composition, acceptable property characteristics and reliable property predictions (using the current DWPF models) are of interest. Comparisons between property predictions and property measurements are provided for these Phase 2 PHA glasses in the discussion that follows.

Glasses were batched and fabricated to the target compositions corresponding to rows pha13 through pha18 of Table 2. In addition to the Phase 2 glasses (both PHA and CST), a standard glass (Batch 1) and a standard uranium-bearing glass were included in the planning of these analyses (for possible bias-correction). An analytical plan (in the form of a memorandum) was provided to assist the SRTC-Mobile Laboratory (SRTC-ML) in conducting these analyses (see Attachment I of [5]). Due to equipment problems, the SRTC-ML was unable to perform these analyses, so these samples were submitted to the Analytical Development Section of SRTC for analysis.

Glasses were batched using the appropriate combinations of Purex sludge, glass formers, PHA, and MST. The simulated Purex sludge was batched from dry chemicals and has an oxide composition provided in Table 3 of Attachment I of [3]. PHA was batched from chemicals and has an oxide

composition provided in Table 2 of Attachment I of [3]. A basic MST solution was obtained from D. Hobbs. This material was washed and then dried. The composition of MST was determined by the SRTC-ML and is presented in Table 1 of Attachment I of [3]. Frit 202, Lot 14 was obtained from the DWPF. The Frit 202 composition is given in Table 7 of Attachment I of [3].

For each glass, the combined powders (~120 grams) were added to a 250 mL Pt-Au crucible and placed in a calibrated furnace, heated to 1150°C at a rate of 10°C/minute, and then held for four hours at 1150°C. The crucible was then removed, and the glass immediately poured onto a clean stainless steel plate.

Tables A.1 and A.2 in the Appendix provide the composition measurements obtained by ADS using a variation of the analytical plan given in Attachment I of [5].¹ Two dissolutions (microwave and peroxide fusion) were used to generate these composition measurements. Table A.1 provides the peroxide fusion (pf) results and Table A.2 the microwave (MW) results. Calcium and silicon cation concentrations were measured using both preparation methods. Exhibit A.1 in the Appendix provides a plot of the measurements by glass sample id by oxide. A review of these plots reveals that one of the microwave dissolutions for pha14 yielded questionable measurements for most of the analytes. In the analyses that follow, these questionable results have been excluded from the computations. The peroxide fusion measurements for CaO are more varied than the measurements for this oxide derived using microwave dissolution. However, none of these CaO measurements were excluded in the analyses that follow.

A review of the results from the standards are used to provide insight into the possibility that the ICP calibration contributes (in a systematic way) to the variation seen in the oxide measurements for the Phase 2 glasses. Exhibit A.2 in the Appendix provides plots of the oxide measurements per analytical block by oxide for those samples prepared using peroxide fusion dissolutions, and Exhibit A.3 in the Appendix provides similar plots for the samples prepared using microwave dissolutions. Table 3 provides the average measured compositions for the two standards included in this analytical plan. The reference values for the standards are also provided in this table.

Table 3: Measurements from Glass Standards

Oxide	std (Batch 1)			Ustd (Uranium-bearing Standard)		
	Analytical Block			Analytical Block		
	1	2	Reference	1	2	Reference
	3 obs	3 obs	Value	2 obs	2 obs	Value
Al ₂ O ₃	4.222	4.278	4.877	3.815	3.898	4.100
B ₂ O ₃	7.670	7.870	7.777	9.097	9.518	9.209
CaO (pf)	1.803	1.795	1.220	2.327	1.800	1.301
CaO (MW)	1.086	1.058	1.220	1.244	1.230	1.301
CaO (avg)	1.444	1.426	1.220	1.785	1.515	1.301
Cr ₂ O ₃	0.106	0.113	0.107	0.264	0.276	0.000
CuO	0.398	0.397	0.399	0.016	0.020	0.000
Fe ₂ O ₃	13.258	13.156	12.839	14.041	14.105	13.196
K ₂ O	3.082	3.168	3.327	2.749	2.900	2.999
Li ₂ O	4.523	4.428	4.429	3.131	3.122	3.057
MgO	1.153	1.168	1.419	1.073	1.100	1.210
MnO	1.657	1.668	1.726	2.764	2.814	2.892
Na ₂ O	8.689	8.630	9.003	11.717	11.765	11.795
Nb ₂ O ₅	0.070	0.090	0.000	0.073	0.073	0.000
NiO	0.781	0.794	0.751	1.137	1.155	1.120
SiO ₂ (pf)	50.264	52.672	50.220	45.469	48.288	45.353
SiO ₂ (MW)	47.369	47.465	50.220	43.854	43.942	45.353
SiO ₂ (avg)	48.816	50.068	50.220	44.662	46.115	45.353
TiO ₂	0.704	0.706	0.677	1.031	1.043	1.049
U ₃ O ₈	0.340	0.342	0.000	2.313	2.479	2.406
ZrO ₂	0.140	0.130	0.098	0.024	0.026	0.000
Sum of Oxides	97.054	98.432	98.869	99.691	101.925	99.687

¹ The samples were dissolved according to the plan, and then ADS LIMS numbers were randomly assigned to the dissolved samples.

The analytical results from the Batch 1 samples were used to bias-correct for a possible ICP calibration effect (a block effect) in the other measurements.² This was accomplished for each oxide in turn by taking the original oxide measurement, noting its block, and then multiplying the measurement by the ratio of the corresponding reference value for Batch 1 divided by the average oxide measurement for Batch 1 in that block. The calcium and silicon values for each dissolution method were adjusted via this process. This approach was used to bias-correct the composition measurements of the Phase 2 and standard glasses for each preparation method.

Exhibit A.4 in the Appendix provides plots of the average measurements for each oxide for each of the glasses (including the standards), and Table 4 provides summary information for these measurements. The sums of oxides for the target, measured, and measured bias-corrected (bc) compositions are also provided. A review of these sums shows that they are all within the interval of 95 to 105 weight percent with the smallest value being 97.8 wt% for the measured composition of pha13 and the largest value being 104.0 for the bias-corrected composition of pha18.

Some observations regarding the plots of Exhibit A.4 are warranted. Bias correction does not move the Al_2O_3 , Na_2O , NiO , or ZrO_2 values toward their respective target levels. The TiO_2 measurements are consistently low for these PHA glasses even though the Batch 1 and uranium-standard measurements are more near their respective targets. The TiO_2 problem was also discussed in [3] where similar behavior for TiO_2 was revealed. Namely, the TiO_2 measurements for the PHA glasses are falling short of their respective target values even though the measurements for the standards compare very favorably to their targets. This behavior prompted a re-evaluation of the major source of TiO_2 , the MST. A subsequent analysis of MST revealed a larger than expected moisture content. However, as discussed in [3], glasses for Phases 1 and 2 were batched and fabricated prior to this discovery. Batching formulations were subsequently modified to account for the additional loss that would be expected for this situation. Glasses for Phases 3 and 4 are to be batched in a manner fully accounting for the loss of the additional moisture. In addition, Phase 4 is to include selected glasses from Phases 1 and 2 that are to be re-batched using the new formulations. This will provide better coverage of the higher MST loadings for these phases of the CST study.

One other pattern revealed in Exhibit A.4 warrants a comment. The measurements for the PHA components (B_2O_3 , CuO , K_2O , and Na_2O) suggest that the batching procedures used to account for the PHA in these glasses led to the targets for B_2O_3 and Na_2O being exceeded while the amounts of CuO and K_2O were correspondingly diluted. These effects are especially evident in pha15 and pha18. A review of the targets versus measurements presented in Table 4 supports the likelihood that the PHA used to batch these glasses may have been inaccurately prepared. Possible effects from this error are identified in the discussion that follows.

² Bias corrections of this type have been advantageous (see for example "A Statistical Review of Data from the SRTC Mobile Laboratory," WSRC-RP-98-00430, Revision 0, June 15, 1998) but not always. In some instances, bias correction does not improve the accuracy of the results. Measurements are bias-corrected in this report, and bias-corrected values are considered in the comparisons that follow. Conclusions, developed from these comparisons, that are insensitive to the way the glass compositions are represented (target, measured, or bias-corrected) demonstrate robustness to which representation might be nearer the true composition for each glass.

Table 4: Target, Measured and Bias-Corrected Compositions (in wt%) for the Phase 2 Glasses

	<i>Batch 1</i>			<i>Uranium Standard (u-std)</i>			<i>pha13</i>		
	Target	Measured	Bias-cor.	Target	Meas.	Bias-cor.	Target	Measured	Bias-cor.
Al ₂ O ₃	4.877	4.250	4.877	4.100	3.856	4.425	3.263	3.246	3.725
B ₂ O ₃	7.777	7.770	7.777	9.209	9.308	9.315	7.345	7.492	7.498
CaO	1.220	1.435	1.220	1.301	1.650	1.403	1.239	1.357	1.196
Cr ₂ O ₃	0.107	0.110	0.107	0.000	0.270	0.264	0.144	0.152	0.149
CuO	0.399	0.398	0.399	0.000	0.018	0.018	0.585	0.573	0.575
Fe ₂ O ₃	12.839	13.207	12.839	13.196	14.073	13.681	13.472	13.615	13.236
K ₂ O	3.327	3.125	3.327	2.999	2.825	3.007	3.380	3.470	3.694
Li ₂ O	4.429	4.476	4.429	3.057	3.126	3.094	4.236	4.214	4.171
MgO	1.419	1.160	1.419	1.210	1.087	1.329	1.314	1.284	1.570
MnO	1.726	1.663	1.726	2.892	2.789	2.895	2.355	2.272	2.359
Na ₂ O	9.003	8.660	9.003	11.795	11.741	12.207	8.363	8.342	8.673
NiO	0.751	0.788	0.751	1.120	1.146	1.093	1.268	1.142	1.089
SiO ₂	50.220	49.442	50.220	45.353	45.388	46.114	47.849	46.844	47.619
TiO ₂	0.677	0.705	0.703	1.049	1.037	1.034	1.125	0.738	0.736
U ₃ O ₈	0.000	0.341	0.341	2.406	2.396	2.396	2.731	2.792	2.792
ZrO ₂	0.098	0.135	0.144	0.000	0.025	0.026	0.149	0.182	0.194
Sum of Oxides	98.869	97.743	99.362	99.687	100.808	102.376	98.818	97.792	99.353
	<i>pha14</i>			<i>pha15</i>			<i>pha16</i>		
	Target	Measured	Bias-cor.	Target	Measured	Bias-cor.	Target	Measured	Bias-cor.
Al ₂ O ₃	3.245	3.120	3.580	3.227	3.116	3.576	3.256	3.266	3.748
B ₂ O ₃	8.174	10.060	10.069	9.003	11.647	11.657	7.246	8.555	8.562
CaO	1.234	1.272	1.132	1.230	1.371	1.204	1.237	1.603	1.370
Cr ₂ O ₃	0.144	0.146	0.143	0.144	0.153	0.150	0.144	0.152	0.149
CuO	0.808	0.739	0.741	1.031	0.959	0.962	0.585	0.549	0.551
Fe ₂ O ₃	13.470	13.851	13.466	13.467	14.684	14.275	13.471	13.805	13.421
K ₂ O	4.760	4.150	4.417	6.140	4.607	4.905	3.379	3.231	3.440
Li ₂ O	4.030	4.006	3.964	3.824	3.766	3.727	4.150	4.237	4.193
MgO	1.255	1.228	1.502	1.195	1.145	1.401	1.289	1.300	1.590
MnO	2.355	2.176	2.259	2.355	2.156	2.239	2.355	2.292	2.380
Na ₂ O	8.511	9.175	9.539	8.659	9.959	10.354	8.438	8.855	9.206
NiO	1.268	1.109	1.057	1.268	1.134	1.081	1.268	1.139	1.086
SiO ₂	45.569	45.191	45.916	43.289	41.318	42.011	46.899	47.632	48.374
TiO ₂	1.123	0.742	0.740	1.122	0.721	0.719	2.223	1.460	1.456
U ₃ O ₈	2.731	2.921	2.921	2.731	1.988	1.988	2.731	2.919	2.919
ZrO ₂	0.149	0.171	0.182	0.149	0.183	0.195	0.149	0.179	0.190
Sum of Oxides	98.826	100.131	101.702	98.834	98.990	100.526	98.820	101.263	102.724
	<i>pha17</i>			<i>pha18</i>					
	Target	Measured	Bias-cor.	Target	Measured	Bias-cor.			
Al ₂ O ₃	3.238	3.146	3.610	3.220	3.057	3.508			
B ₂ O ₃	8.075	9.512	9.520	8.904	11.880	11.890			
CaO	1.233	1.374	1.203	1.228	1.442	1.247			
Cr ₂ O ₃	0.144	0.149	0.146	0.144	0.149	0.145			
CuO	0.808	0.741	0.744	1.031	0.960	0.963			
Fe ₂ O ₃	13.469	13.834	13.449	13.466	14.339	13.940			
K ₂ O	4.759	4.547	4.841	6.139	4.895	5.209			
Li ₂ O	3.945	3.981	3.940	3.739	3.825	3.786			
MgO	1.230	1.176	1.438	1.170	1.155	1.412			
MnO	2.355	2.344	2.434	2.355	2.125	2.206			
Na ₂ O	8.586	9.104	9.465	8.734	10.049	10.447			
NiO	1.268	1.154	1.101	1.268	1.101	1.050			
SiO ₂	44.619	44.669	45.383	42.339	42.640	43.350			
TiO ₂	2.221	1.449	1.445	2.220	1.460	1.456			
U ₃ O ₈	2.731	2.487	2.487	2.731	3.091	3.091			
ZrO ₂	0.149	0.169	0.180	0.149	0.206	0.221			
Sum of Oxides	98.830	99.910	101.457	98.837	102.451	103.997			

PCT Results

The six PHA glasses making up Phase 2, after being batched and fabricated, were subjected to the 7-day Product Consistency Test (PCT) as an assessment of their durabilities [4]. More specifically, Method A of PCT (ASTM C1285) was used for these measurements. Since durability is a critical product quality metric for vitrified nuclear waste, a review of the PCTs for these glasses was seen as a prerequisite for additional testing of these glasses. The PCTs were conducted in triplicate for the Phase 2 glasses. In addition, PCTs were also conducted in triplicate for samples of the Environmental Assessment (EA) glass, the ARM glass, and a reagent blank. An analytical plan supporting these tests was provided in the form of a memorandum (see Attachment II of [5]). This plan assisted the SRTC-ML in measuring the compositions of the solutions resulting from these PCTs. Of primary interest were the concentrations (in parts per million, ppm) of boron (B), lithium (Li), sodium (Na), and silicon (Si). Samples of a multi-element solution standard were also included in this analytical plan (as a check on the accuracy of the Inductively Coupled Plasma (ICP) – Emission Spectrometer used for these measurements).

The results from these tests are given in Table A.3 of the Appendix. Any measurement determined to be below detection was replaced by $\frac{1}{2}$ of the detection limit in subsequent analyses. PCT leachate concentrations are typically normalized using the cation composition (expressed as a weight percent) in the glass to obtain a grams-per-liter (g/L) leachate concentration. The normalization of the PCTs is usually conducted using the measured compositions of the glasses. This is the preferred normalization process for the PCTs. For completeness, the target cation compositions will also be used to conduct this normalization.

As is the usual convention, the common logarithm of the normalized PCT (normalized leachate, NL) for each element of interest will be determined and used for comparisons. To accomplish this computation, one must

1. Determine the common logarithm of the elemental parts per million (ppm) leachate concentration for each of the triplicates and each of the elements of interest (these values are provided in Table A.3 of the Appendix),
2. Average the common logarithms over the triplicates for each element of interest, and then

Normalizing Using Measured Composition (preferred method)

3. Subtract a quantity equal to 1 plus the common logarithm of the average cation measured concentration (expressed as a weight percent of the glass) from the average computed in step 2.

Or

Normalizing Using Target Composition

3. Subtract a quantity equal to 1 plus the common logarithm of the target cation concentration (expressed as a weight percent of the glass) from the average computed in step 2.

As a preliminary step to completing these normalizations of the PCTs, a review of the data was conducted. Exhibit A.5 in the Appendix provides plots of the leachate concentrations by sample id and by element with and without the EA and blank samples. No problems are seen in these data, in that the results are reasonably consistent across all Phase 2 and standard glasses. Table 5 provides a look at the results from the three analyses of the multi-element standard solution that were included in each block of the analytical plan. These results also indicate consistent and reasonably accurate results from these analyses.

Table 5: Measurements of Standard Solution

Block	Sequence	B (ppm)	Si (ppm)	Na (ppm)	Li (ppm)
1	1	20.5	49.5	83.0	10.3
1	2	19.8	48.7	80.9	9.8
1	3	21.1	47.6	82.2	9.7
Block 1	average	20.5	48.6	82.0	9.9
2	1	20.3	48.9	85.3	9.6
2	2	22.4	48.8	83.2	9.5
3	3	20.5	47.6	85.0	9.1
Block 2	average	21.1	48.4	84.5	9.4
3	1	20.1	50.4	86.4	10.6
3	2	20.2	48.1	84.4	10.3
3	3	22.2	47.5	82.3	9.9
Block 3	average	20.8	48.7	84.4	10.3
Overall	average	20.8	48.6	83.6	9.9
Reference	Value	20	50	81	10
% Difference		3.9%	-2.9%	3.3%	-1.2%

Table 6 provides the results from the normalization process using the information in Table 4 and Table A.3. Exhibit A.6 in the Appendix provides scatter plots for these results offering an opportunity to investigate the consistency in the leaching across the elements for the glasses of this study. This consistency is typically demonstrated by a high degree of linear correlation among the values. The PCTs normalized using the target, measured, or bias-corrected compositions all show a high degree of linear correlation. All of these correlations are greater than 99%.

Table 6: Normalized PCT's

Glass ID	Composition	log NL [B (g/L)]	log NL [Si (g/L)]	log NL [Na (g/L)]	log NL [Li (g/L)]	NL B (g/L)	NL Si (g/L)	NL Na (g/L)	NL Li (g/L)
ARM	reference comp. [7]	-0.27166	-0.55545	-0.26983	-0.20863	0.53	0.28	0.54	0.62
EA	reference comp. [7]	1.27261	0.61353	1.17131	1.02046	18.73	4.11	14.84	10.48
cst13	measured	0.00224	-0.29231	-0.00987	-0.01053	1.01	0.51	0.98	0.98
	measured, bias-cor.	0.00188	-0.29945	-0.02678	-0.00603	1.00	0.50	0.94	0.99
	target	0.01087	-0.30154	-0.01099	-0.01280	1.03	0.50	0.98	0.97
cst14	measured	0.19248	-0.22405	0.14767	0.14326	1.56	0.60	1.40	1.39
	measured, bias-cor.	0.19210	-0.23097	0.13078	0.14782	1.56	0.59	1.35	1.41
	target	0.28267	-0.22767	0.18031	0.14062	1.92	0.59	1.51	1.38
cst15	measured	1.03756	0.10905	0.90759	0.87170	10.90	1.29	8.08	7.44
	measured, bias-cor.	1.03719	0.10183	0.89070	0.87621	10.89	1.26	7.77	7.52
	target	1.14941	0.08882	0.96835	0.86498	14.11	1.23	9.30	7.33
cst16	measured	0.02870	-0.28244	0.00482	0.01993	1.07	0.52	1.01	1.05
	measured, bias-cor.	0.02834	-0.28916	-0.01207	0.02446	1.07	0.51	0.97	1.06
	target	0.10080	-0.27571	0.02577	0.02890	1.26	0.53	1.06	1.07
cst17	measured	0.28994	-0.16319	0.24903	0.24200	1.95	0.69	1.77	1.75
	measured, bias-cor.	0.28957	-0.17007	0.23213	0.24650	1.95	0.68	1.71	1.76
	target	0.36106	-0.16270	0.27445	0.24597	2.30	0.69	1.88	1.76
cst18	measured	1.04580	0.12882	0.92094	0.89664	11.11	1.35	8.34	7.88
	measured, bias-cor.	1.04544	0.12165	0.90405	0.90118	11.10	1.32	8.02	7.96
	target	1.17103	0.13189	0.98185	0.90659	14.83	1.35	9.59	8.06

As seen in Table 6, the durabilities for most of the PHA Phase 2 glasses are much better than that of EA. (This is indicated for each glass by its normalized leachate being much smaller than that of EA.) Figure 1 provides an opportunity for a closer look at these results using measured and bias-corrected compositions. Figure 1 is a plot of the DWPF model that relates the logarithm of the normalized PCT (in this case for B) to a linear function of a free energy of hydration term, ΔG_p (kcal/100g glass), derived from the glass (measured and bias-corrected) compositions [7]. Prediction limits (at 95% confidence) for individual PCT results are also plotted around this linear fit. The PCT results for EA (shown as a diamond), ARM (shown as a "z"), and the PHA glasses (each shown as an "x") are presented on this plot. Note that the PHA results reveal that all glasses except pha15 and pha18 are predicted well by the current DWPF durability model. In addition, the limit for the PCCS property acceptance region for durability (determined from the relationship shown in Figure 1) is a value for ΔG_p of -12.82 [8] (i.e., for a glass composition to be acceptable from a PCCS boron durability perspective, its ΔG_p must be greater than -12.82). Thus, even though both glasses leached less than

EA, their free energy of hydration values (based upon the measured and bias-corrected compositions) fall outside the acceptance region for boron durability. Figure 2 provides a plot of the boron results based upon target compositions. Exhibit A.7 in Appendix provides similar plots of the PHA durability measurements versus the DWPF durability models for B, Si, Na, and Li. The behaviors seen in the plots for Si, Na, and Li are similar to that demonstrated by the B results: all PHA Phase 2 glasses except pha15 and pha18 are durable and predictable.

Figure 1.
Log NL(B) (g/L) By del Gp
(Using PHA Measured & Bias-corrected compositions and
EA and ARM reference compositions)

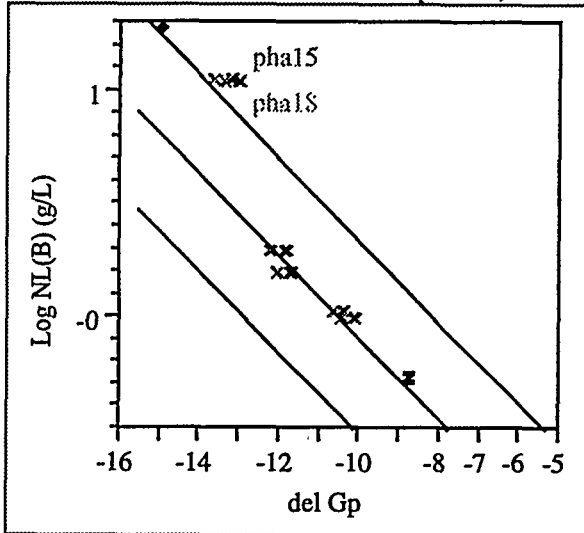
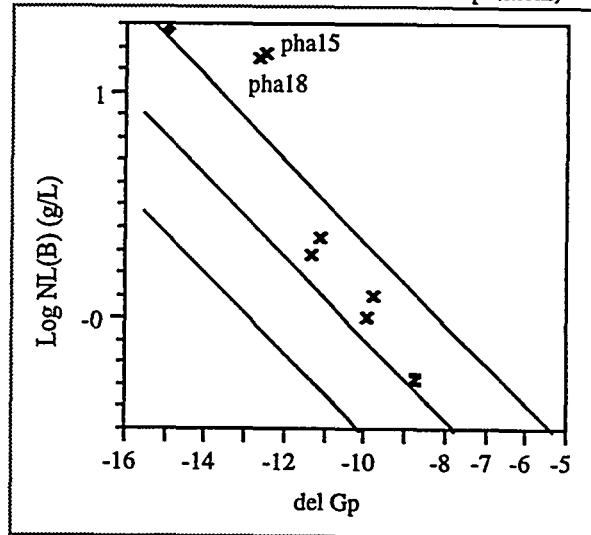


Figure 2.
Log NL(B) (g/L) By del Gp
(Using PHA target compositions &
EA and ARM reference compositions)



As previously discussed, the measurements of the compositions for pha15 and pha18 indicate that the levels of boron and sodium in these two glasses far exceeded their respective target concentrations (by 14 to 33%, see Table 4 for details). This is also true for the compositions of the other PHA Phase 2 glasses, although the problem is more severe in pha15 and pha18, the glasses targeted to contain the most PHA. Note, however, that the durability models do well in predicting the PCTs for the other glasses. Knowing that these models were developed to represent durabilities for only homogeneous glasses [7], the possibility that pha15 and pha18 may be phase-separated cannot be excluded. Phase separation for these PHA Phase 2 glasses is discussed below.

Viscosity at 1150 °C

Viscosity measurements for a subset of these Phase 2 glasses were conducted at SRTC using a Harrop, high-temperature viscometer [9]. The viscosity (in Poise) of each of these glasses at 1150 °C was to be estimated from a Fulcher equation fitted to a set of viscosity measurements taken over an appropriate range of temperatures. The functional form of the (three-parameter) Fulcher equation (expressed in Poise) used to fit these data is given by equation (1):

$$\ln \hat{\eta} = A + \frac{B}{(T - C)} \quad (1)$$

where A, B, and C represent the parameters of the model that are to be determined from the available measurements (represented by $\hat{\eta}$, expressed in Poise) at various temperatures (represented by T). The fitted model is then used to predict the viscosity of the given glass at 1150 °C.

Although no definitive error analysis has been conducted on the use of this Harrop viscometer, SRTC has conducted several sets of viscosity measurements using this viscometer with good results [10]. The original plan (see Attachment III of [5]) for studying the viscosities of these Phase 2 glasses called for measurements to be made on all six glasses. Two crucible/spindle sets were to be used in conducting these measurements. This plan covered the CST and PHA Phase 2 glasses and called for these measurements to be followed by measurements of the Batch 1 standard glass with both crucible/spindle sets. Other measurements of Batch 1 conducted before the planned measurements were reported in as part of the Phase 1 results [3]. Due to a problem with the crucible fouling during some of these measurements, the plan for measuring these viscosities was modified (see Attachment IV of [5]); and measurements were completed for only four glasses, pha14, pha15, pha17, and pha18. Exhibit A.8 of the Appendix provides the measured viscosities, the results of the Fulcher fit, and the prediction at 1150°C for these four PHA Phase 2 glasses. The information presented in this exhibit (along with predictions from the DWPF viscosity model and the Batch 1 results from [10] and [3]) is summarized in Table 7.

Table 7: Viscosity Results (in Poise) By Glass ID

Glass ID	Viscosity (Poise) @ 1150°C	Predicted (measured composition)	Predicted (bias-corrected composition)	Predicted (target composition)
Batch 1	48.6, 49.7, 46.4 48.9, 47.3	44.2 (Sharp-Schurtz) ³		56.2
pha13	Not Measured	42.4	45.4	46.7
pha14	22.8	26.6	28.3	33.3
pha15	14.8	13.6	14.6	23.0
pha16	Not Measured	39.4	42.1	44.2
pha17	22.2	25.8	27.4	31.3
pha18	15.0	14.9	15.8	21.3

The measured melt viscosities at 1150°C for these four PHA glasses are very near or below the operating range for DWPF [8]. This is not unexpected for glasses with this high level of PHA. The current DWPF viscosity model performs well in predicting these results.

Liquidus Temperature (T_L)

The standard ASTM procedure for measuring liquidus temperature uses a gradient furnace. The equipment for determining liquidus temperature by this method is being installed and tested within SRTC in a clean laboratory. Due to the presence of depleted uranium in the glass samples (as well as the early stage of equipment setup), we were not able to use this method for liquidus determination. A decision was therefore made to perform isothermal holds using reasonable quantities of the glass to bound the liquidus temperature.

XRD was selected as the method of detection for crystal formation in the glasses after an isothermal hold. It is estimated that the sensitivity of XRD (non-quantitative) is ~ 0.7 to 1 wt% for a crystalline phase (in this case, Trevorite [11]). Therefore, for this type of measurement, absence of detection of a crystalline phase was evidence that the liquidus temperature is less than the temperature of that isothermal hold. On the other hand, detection of Trevorite (or any other primary crystalline phase) indicates that the liquidus temperature is higher than the temperature of the isothermal hold.

The liquidus temperature for each glass composition was bounded by performing isothermal holds at 900°C, 950°C, 1000°C, and 1050°C. Approximately 5 grams of glass were placed in a small platinum crucible and transferred to a furnace already heated to 1150°C. After a four-hour hold period, the temperature was reduced to 900°C, 950°C, 1000°C, or 1050°C and held at that temperature for 24 hours. The crucible was then removed from the furnace and the glass allowed to cool within the crucible at room temperature. For these experiments, twelve glasses were treated together. The twelve

³

Sharp-Schurtz is the analytic arm of Owens Corning Fiberglas and is now known as Owens Corning Testing (OCT).

glasses consisted of the six CST and six PHA glasses containing 30 wt% Purex simulated sludge. Therefore, the CST and PHA glasses experienced essentially identical heat treatments. The six PHA glasses at 900°C were submitted for XRD analysis. Care was taken to obtain glass that was not part of the top glass surface. The glass pieces, although mainly from the bulk, usually included part of the bottom surface (i.e., that surface in contact with the crucible).

The XRD analysis demonstrated that none of the glasses had crystals after a 24 hold at 900°C. Therefore, the bounding liquidus temperatures for these glasses are:

Table 8: Liquidus Temperatures

<u>GLASS ID</u>	<u>LIQUIDUS TEMPERATURE</u>
pha13	<900°C
pha14	<900°C
pha15	<900°C
pha16	<900°C
pha17	<900°C
pha18	<900°C

The bounding liquidus temperatures are below the nominal property acceptance region (PAR) value of 1025°C [8] and are therefore expected to meet DWPF processing requirements for liquidus. The model predictions for these six glasses ranged from 1033°C to 1066°C using targeted chemical compositions, from 1040°C to 1096°C using measured compositions, and 1033 °C to 1088 °C using bias-corrected compositions. Therefore, the models predict unacceptable liquidus temperatures using the measured compositions of these glasses.

Surface Crystallization

For liquidus measurements, crystal formation is considered only in the interior glass region. Therefore, samples submitted for XRD analysis were bulk samples. However, crystals can form at the interface of the glass and the crucible and/or the glass and air. For completeness, the detection of these surface crystals on the top of the glass is provided in Table 9 as a function of temperature.

Table 9. Surface Crystals for the Six PHA Glasses as a Function of Temperature

----after the 24 hour heat treatment----

	pha13	pha 14	pha 15	pha 16	pha 17	pha 18
1150°C	none	none	none	none	none	none
1000°C	none	none	none	none	none	none
950°C	none	none	none	none	none	none
900°C	none	none	none	none	none	none

As shown in the table, surface crystallization was not detected for any of these glasses heat-treated at any of these temperatures.

Phase Separation

The formation of separate amorphous phases in the glass is referred to as amorphous phase separation or inhomogeneity. Crystal formation, as determined by liquidus measurements, on the other hand is also a type of phase separation, but reflects crystalline particles within the glass matrix. Amorphous phase separation is to be avoided since the models currently used to predict durability do not apply for glasses predicted to be phase separated. The property acceptance region (PAR) limit for the homogeneity constraint in the PCCS is nominally a value of 211 [8]. For the measurement acceptance region (MAR), the value will be even higher. In order to pass this constraint, the calculated value must be greater than the MAR value. These values are provided in Table 10. All of these compositions (target, measured, and bias-corrected) satisfy the PAR for homogeneity. It is beyond the scope of the study, to determine whether or not the homogeneity MAR is satisfied.

Table 10: Homogeneity Property Predictions
(A Composition is in the PAR if its prediction is greater than 211)

Glass ID	Homogeneity Property Prediction based on		
	Target Composition	Measured Composition	Bias-Corrected Composition
pha13	215.6	215.7	217.5
pha14	215.3	219.4	221.2
pha15	214.9	222.6	224.1
pha16	213.9	221.7	223.0
pha17	213.5	218.8	220.4
pha18	213.2	223.9	225.3

The homogeneity constraint was developed for glasses that do contain PHA. Therefore, the predictability of phase separation by this model should be correct for most of these glasses. Recall that the durabilities for glasses pha15 and pha18 were unacceptable and unpredictable (by the current DWPF models). The homogeneity predictions, based upon measured and bias-corrected compositions, suggest that these two glasses are the least likely to be phase-separated out of these Phase 2 glasses. If the homogeneity model is correct for this compositional range, it is unclear why glasses pha15 and pha18 were unacceptable. A significant search for phase separation in these glasses is beyond the scope of work for this task, except when routine SEM analysis is performed. For these six glasses no SEM analyses were performed.

CONCLUSIONS

The results presented in this report are for six Phase 2 PHA glasses, each of which was targeted to contain 30 wt% simulated PUREX sludge on an oxide basis. The target PHA concentration was varied from 7 to 10 to 13 wt % oxides both at 1.25 and 2.5 wt % oxides of washed MST. However, the PHA targets were not achieved.

The results of the chemical composition analyses of the PHA Phase 2 glasses revealed a significant problem with certain elements. Both boron and sodium were higher than the target values, whereas potassium and copper were less than the target values. This suggested a problem with batching of the PHA for this phase. An analysis of the data, in which several different scenarios were considered and then tested by calculation, revealed that the probable cause was the use of anhydrous sodium borate rather than the intended hydrated sodium borate. The measured values are both qualitatively and quantitatively consistent with this error.

A recovery from this error was made by rebatching and melting glasses pha14, pha15, pha17, and pha18. The results will be included in Phase 4, PHA report. It was decided to report the results for the current glasses, even though they missed the target, since they provide additional insight into the durability of the PHA glasses. The viscosity results provide evidence for the predictability of the viscosity model at these high PHA loadings that have very low viscosity values.

Only four of the six glasses were durable when compared to the EA glass (as determined by the 7-day PCT). Glasses pha15 and pha18, with the highest level of PHA, were not durable and were outside the limits of predictability. Both glasses leached less than EA but their measured compositions led to these glasses not falling within the acceptance region for durability as established by DWPF's PCCS. Although the PHA target was not achieved, a relatively small increase in boron and sodium over that targeted resulted in failure of the glasses from a PCT perspective. This result leads to a caution for all the results obtained from both variability studies (PHA and CST). The current studies selected fixed points in compositional space and did not permit variation in the compositions of each element independently. As one increases the variability of elements and fabricates and tests the resultant glasses, a threshold usually appears. Passing this threshold can lead to poor glass quality or unacceptable processing parameters. Thus, the size of the actual processing window is not revealed

from this type of study. On the other hand, the inadvertent production of pha15 and pha18 glasses provides evidence that such a threshold does exist for these glasses.

All six glasses passed the homogeneity constraint indicating that amorphous phase separation should not be an issue. It is not clear what the mechanism is for the durability failure of glasses pha15 and pha18, but the homogeneity model used by PCCS to screen for phase separation, if correct, points to some other cause.

The models currently in PCCS were also used to calculate liquidus and viscosity for these six glasses. The viscosity model appears to work well at predicting the very low viscosities measured for these glasses. The viscosity values were either below or close to the lower limit of 20 poise for operation at DWPF. The viscosity model is not conservative to the lower limit (i.e., the predicted viscosities are not less than the measured viscosities). No crystallization was observed for these glasses even though the models predicted that the liquidus temperatures would be mostly unacceptable for these compositions.

REFERENCES

- [1] Elder, H. H., "Technical Task Request: DWPF Waste Qualification – DWPF Coupled Operation Chemistry," HLW-SDT-TTR-99-07.0, February 2, 1999.
- [2] Harbour, J. R. and T. B. Edwards, "Technical Task and QA Plan: DWPF Coupled Operation Chemistry – PHA Glass Testing," WSRC-RP-99-00218, Revision 1, April 23, 1999.
- [3] Edwards, T. B., J. R. Harbour, and R. J. Workman, "Composition and Property Measurements for PHA Phase 1 Glasses (U)," WSRC-TR-99-00262, Revision 0, August 4, 1999.
- [4] ASTM C1285-94, "Standard Test Methods for Determining Chemical Durability of Nuclear Waste Glasses: The Product Consistency Test (PCT)," 1994.
- [5] Edwards, T. B., J. R. Harbour, and R. J. Workman, "Composition and Property Measurements for CST Phase 2 Glasses (U)," WSRC-TR-99-00289, Revision 0, August 18, 1999.
- [6] Harbour, J. R. and T. B. Edwards, "Analytical Study Plan-PHA: DWPF Coupled Operation Chemistry – PHA Glass Testing," WSRC-RP-99-00315, Revision 0, April 14, 1999.
- [7] Jantzen, C. M., J. B. Pickett, K. G. Brown, T. B. Edwards, and D. C. Beam, "Process/Product Models for the Defense Waste Processing Facility (DWPF): Part I. Predicting Glass Durability from Composition Using a Thermodynamic Hydration Energy Reaction Model (THERMO) (U)," WSRC-TR-93-672, Rev. 1, September 28, 1995.
- [8] Brown, K. G. and R. L. Postles, "SME Acceptability Determination for DWPF Process Control (U)," WSRC-TR-95-0364, Revision 3, February 21, 1996.
- [9] Schumacher, R. F. and D. K. Peeler, "Establishment of Harrop, High-Temperature Viscometer," WSRC-RP-98-00737, Revision 0, September 1998.
- [10] Schumacher, R. F., R. J. Workman, J. R. Harbour, and T. B. Edwards, "Measurements of DWPF Glass Viscosity – Interim Report," WSRC-RP-99-00350, Revision 0, May 5, 1999.
- [11] Cicero, C. A., S. L. Marra, and M. K. Andrews, "Phase Stability Determinations of DWPF Waste Glasses (U)," WSRC-TR-93-227, Revision 0, 1993.

This page intentionally left blank.

Appendix:

Supplemental Tables and Exhibits

This page intentionally left blank.

**Table A.1: Composition Measurements from Peroxide Fusion Preparation
(expressed as cation weight fractions)**

Peroxide Fusion Dissolution – ICP ES							
Glass ID	Block	Seq	LIM #	Lab ID	B	Ca	Si
Batch 1	1	1	130894a	Na2O2-Batch 1 std-1	0.02219	0.01073	0.21868
Batch 1	1	15	130895a	Na2O2- Batch 1 std-2	0.02488	0.01431	0.24235
Batch 1	1	29	130896a	Na2O2- Batch 1 std-3	0.02438	0.01362	0.24384
Batch 1	2	1	130894b	Na2O2- BATCH 1 STD-1	0.02308	0.01425	0.23059
Batch 1	2	15	130895b	Na2O2- Batch 1 std-2	0.02498	0.01208	0.25224
Batch 1	2	29	130896b	Na2O2- Batch 1 std-3	0.02527	0.01215	0.25580
Ustd	1	8	130897a	Na2O2- U std-1	0.02857	0.01984	0.21343
Ustd	1	22	130898a	Na2O2- U std-2	0.02793	0.01342	0.21166
Ustd	2	8	130897b	Na2O2- U std-1	0.02916	0.01402	0.22139
Ustd	2	22	130898b	Na2O2- U std-2	0.02996	0.01171	0.23005
pha13	1	9	130882a	Na2O2- D07pf2	0.02433	0.01178	0.23129
pha13	1	21	130873a	Na2O2- D07pfl	0.02141	0.00924	0.20364
pha13	2	19	130873b	Na2O2- D07pfl	0.02232	0.01037	0.21532
pha13	2	28	130882b	Na2O2- D07pf2	0.02502	0.01186	0.24316
pha14	1	7	130878a	Na2O2- D11pf2	0.03113	0.01007	0.21496
pha14	1	10	130871a	Na2O2- D11pfl	0.03050	0.00972	0.21171
pha14	2	7	130871b	Na2O2- D11pfl	0.03109	0.00982	0.21885
pha14	2	20	130878b	Na2O2- D11pf2	0.03227	0.00963	0.22792
pha15	1	5	130889a	Na2O2- D12pf2	0.03782	0.01260	0.20194
pha15	1	26	130885a	Na2O2- D12pfl	0.03345	0.00917	0.18080
pha15	2	10	130885b	Na2O2- D12pfl	0.03465	0.01249	0.19042
pha15	2	24	130889b	Na2O2- D12pf2	0.03877	0.00996	0.21160
pha16	1	16	130886a	Na2O2- D09pfl	0.02642	0.01227	0.22910
pha16	1	19	130892a	Na2O2- D09pf2	0.02583	0.02303	0.22603
pha16	2	12	130892b	Na2O2- D09pf2	0.02672	0.01139	0.23647
pha16	2	18	130886b	Na2O2- D09pfl	0.02730	0.00974	0.23895
pha17	1	13	130877a	Na2O2- D02pf2	0.02885	0.01228	0.20935
pha17	1	20	130876a	Na2O2- D02pfl	0.02928	0.01220	0.21313
pha17	2	6	130877b	Na2O2- D02pf2	0.02977	0.01001	0.21912
pha17	2	27	130876b	Na2O2- D02pfl	0.03027	0.01040	0.22309
pha18	1	3	130875a	Na2O2- D10pfl	0.03616	0.01134	0.19637
pha18	1	23	130888a	Na2O2- D10pf2	0.03639	0.01129	0.19874
pha18	2	23	130888b	Na2O2- D10pf2	0.03730	0.01097	0.20651
pha18	2	26	130875b	Na2O2- D10pfl	0.03773	0.01543	0.20991

Measurements at their detection limits were given values equal to the detection limits.

The measurements for the CST Phase 2 glasses that were conducted with these measurements are not shown here.
See [5] for a complete listing of these data.

Table A.2: Composition Measurements From Microwave Preparation
(expressed as cation weight fractions)

Glass	ICP-ES																		AA ⁴
ID	Block	Seq	LIMS #	Lab ID	Al	Ca	Cr	Cu	Fe	Li	Mg	Mn	Na	Ni	Si	Ti	U	Zr	K
Batch 1	1	1	130505a	BATCH 1 STD-1	0.02188	0.00764	0.00076	0.00323	0.09234	0.02116	0.00673	0.01288	0.06371	0.00616	0.21169	0.00427	0.00280	0.00157	0.02524
Batch 1	1	15	130506a	BATCH 1 STD-2	0.02189	0.00755	0.00074	0.00320	0.09325	0.02099	0.00678	0.01286	0.06372	0.00621	0.22757	0.00426	0.00285	0.00081	0.02567
Batch 1	1	29	130507a	BATCH 1 STD-3	0.02325	0.00810	0.00068	0.00312	0.09260	0.02088	0.00734	0.01275	0.06595	0.00605	0.22500	0.00414	0.00302	0.00072	0.02583
Batch 1	2	1	130505B	MW BATCH 1 STD-1	0.02181	0.00727	0.00077	0.00314	0.08993	0.02027	0.00667	0.01268	0.06192	0.00615	0.20998	0.00418	0.00284	0.00122	0.02643
Batch 1	2	15	130506b	MW BATCH 1 STD-2	0.02210	0.00738	0.00077	0.00319	0.09278	0.02078	0.00689	0.01299	0.06373	0.00627	0.22745	0.00427	0.00285	0.00082	0.02615
Batch 1	2	24	130507b	MW BATCH1 STD-3	0.02402	0.00803	0.00078	0.00318	0.09334	0.02066	0.00757	0.01309	0.06641	0.00630	0.22817	0.00424	0.00302	0.00085	0.02632
Ustd	1	8	130508a	U STD-1	0.02042	0.00888	0.00184	0.00014	0.09849	0.01448	0.00658	0.02160	0.08593	0.00903	0.20393	0.00620	0.01835	0.00023	0.02263
Ustd	1	22	130509a	U STD-2	0.01996	0.00890	0.00177	0.00011	0.09792	0.01460	0.00637	0.02122	0.08791	0.00885	0.20606	0.00616	0.02088	0.00013	0.02301
Ustd	2	8	130508b	MW U STD-1	0.02081	0.00873	0.00190	0.00018	0.09857	0.01442	0.00671	0.02186	0.08608	0.00912	0.20276	0.00624	0.02112	0.00023	0.02410
Ustd	2	23	130509b	MW U STD-2	0.02045	0.00885	0.00188	0.00014	0.09875	0.01458	0.00656	0.02172	0.08848	0.00904	0.20805	0.00626	0.02092	0.00016	0.02405
pha13	1	24	130496a	D07MW-1	0.01692	0.00864	0.00100	0.00456	0.09531	0.01971	0.00767	0.01737	0.06191	0.00881	0.21472	0.00438	0.02355	0.00124	0.02897
pha13	1	5	130504a	D07MW-2	0.01681	0.00861	0.00102	0.00454	0.09388	0.01944	0.00756	0.01740	0.06098	0.00884	0.20909	0.00438	0.02287	0.00145	0.02721
pha13	2	17	130496b	MW D07MW-1	0.01797	0.00877	0.00111	0.00471	0.09833	0.02002	0.00810	0.01821	0.06386	0.00933	0.22271	0.00458	0.02616	0.00138	0.03019
pha13	2	14	130504b	MW D07MW-2	0.01700	0.00830	0.00103	0.00449	0.09340	0.01911	0.00764	0.01742	0.06077	0.00891	0.21181	0.00436	0.02213	0.00132	0.02887
pha14	1	16	130486a	D11MW-1	0.00858	0.00461	0.00045	0.00283	0.04607	0.00881	0.00372	0.00792	0.03691	0.00412	0.09217	0.00209	0.01178	0.00081	0.01779
pha14	1	26	130488a	D11MW-2	0.01625	0.00846	0.00095	0.00595	0.09730	0.01887	0.00734	0.01671	0.06841	0.00862	0.20488	0.00443	0.02358	0.00122	0.03360
pha14	2	13	130488b	MW D11MW-2	0.01678	0.00828	0.00105	0.00586	0.09646	0.01834	0.00747	0.01700	0.06772	0.00881	0.20338	0.00446	0.02595	0.00132	0.03530
pha14	2	26	130486b	MW D11W-1	0.00920	0.00449	0.00052	0.00287	0.04680	0.00879	0.00384	0.00816	0.03741	0.00431	0.10179	0.00217	0.01170	0.00069	0.01653
pha15	1	10	130492a	D12MW-1	0.01638	0.00853	0.00104	0.00751	0.10287	0.01742	0.00683	0.01659	0.07332	0.00886	0.19255	0.00430	0.01583	0.00129	0.03796
pha15	1	6	130503a	D12MW-2	0.01664	0.00875	0.00106	0.00811	0.10373	0.01764	0.00694	0.01685	0.07456	0.00907	0.19078	0.00436	0.01718	0.00138	0.03685
pha15	2	27	130492b	MW D12MW-1	0.01649	0.00844	0.00103	0.00755	0.10315	0.01766	0.00696	0.01674	0.07425	0.00887	0.19325	0.00435	0.01755	0.00130	0.03897
pha15	2	2	130503B	MW D12MW-2	0.01645	0.00842	0.00106	0.00746	0.10108	0.01725	0.00689	0.01662	0.07340	0.00884	0.18377	0.00429	0.01686	0.00145	0.03921
pha16	1	19	130481a	D09MW-1	0.01691	0.00881	0.00100	0.00435	0.09582	0.01964	0.00769	0.01740	0.06514	0.00876	0.20975	0.00865	0.02381	0.00128	0.02661
pha16	1	20	130490a	D09MW-2	0.01714	0.00884	0.00102	0.00442	0.09760	0.01997	0.00782	0.01772	0.06613	0.00896	0.21537	0.00880	0.02399	0.00128	0.02662
pha16	2	3	130481B	MW D09MW-1	0.01740	0.00889	0.00106	0.00439	0.09564	0.01956	0.00789	0.01784	0.06552	0.00896	0.20984	0.00874	0.02496	0.00139	0.02710
pha16	2	11	130490b	MW D09MW-2	0.01769	0.00867	0.00110	0.00439	0.09720	0.01955	0.00797	0.01804	0.06597	0.00912	0.21572	0.00882	0.02626	0.00135	0.02695
pha17	1	27	130497a	D02MW-1	0.01717	0.00872	0.00102	0.00599	0.09826	0.01871	0.00735	0.01820	0.06866	0.00911	0.20321	0.00873	0.02161	0.00122	0.03712
pha17	1	28	130499a	D02MW-2	0.01564	0.00809	0.00098	0.00583	0.09533	0.01825	0.00665	0.01769	0.06576	0.00884	0.19954	0.00854	0.02058	0.00119	0.03724
pha17	2	7	130497b	MW D02MW-1	0.01762	0.00876	0.00108	0.00598	0.09766	0.01866	0.00750	0.01863	0.06920	0.00926	0.20133	0.00881	0.02190	0.00134	0.03891
pha17	2	22	130499b	MW D02MW-2	0.01618	0.00809	0.00102	0.00588	0.09580	0.01834	0.00686	0.01810	0.06651	0.00908	0.20164	0.00868	0.02028	0.00126	0.03771
pha18	1	2	130487a	D10MW-1	0.01634	0.00866	0.00099	0.00789	0.10248	0.01836	0.00707	0.01676	0.07653	0.00871	0.20397	0.00898	0.02732	0.00173	0.03627
pha18	1	3	130489a	D10MW-2	0.01571	0.00829	0.00098	0.00758	0.09809	0.01753	0.00676	0.01611	0.07309	0.00843	0.18239	0.00855	0.02645	0.00150	0.04037
pha18	2	10	130487b	MW D10MW-1	0.01653	0.00835	0.00106	0.00769	0.10172	0.01782	0.00711	0.01674	0.07528	0.00881	0.21314	0.00889	0.02662	0.00127	0.04409
pha18	2	29	130489b	MW D10MW-2	0.01615	0.00813	0.00104	0.00752	0.09888	0.01736	0.00691	0.01623	0.07328	0.00866	0.18350	0.00859	0.02447	0.00160	0.04182

Measurements at their detection limits were given values equal to the detection limits.
PHA Phase 2 glasses are provided in this table but not analyzed in this report.

⁴ The potassium values were generated via Atomic Absorption (AA).

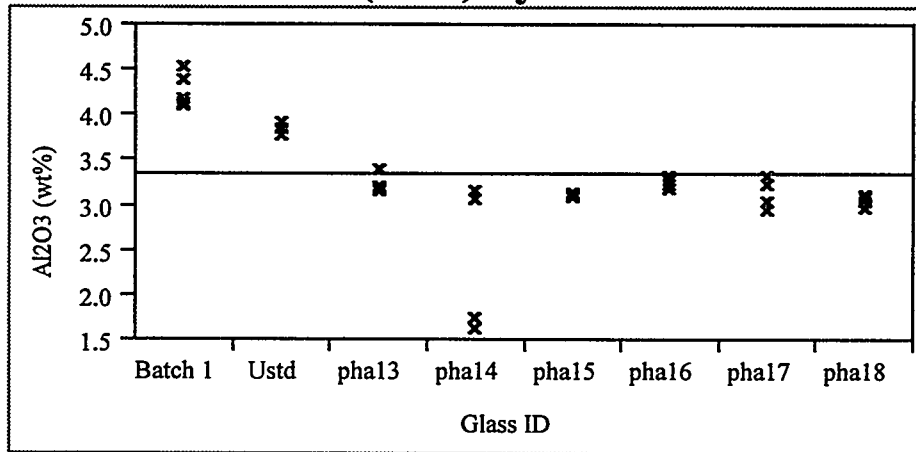
Glass ID	Lab ID					Concentrations in ppm (as reported)				Concentrations in ppm (after correcting for dilution)				Common Logarithm of ppm Concentrations			
		Blk	Seq	B		Si	Na	Li	B	Si	Na	Li		log[B]	log[Si]	log[Na]	log[Li]
std	std-b1-1	1	1	20.5		49.5	83	10.3	20.5	49.5	83.0	10.3		1.3118	1.6946	1.9191	1.0128
blank	y05	1	3	<0.180		0.223	<0.530	<0.010	0.2	0.4	0.4	0.0		-0.8239	-0.4298	-0.3549	-2.0792
pha17	y06	1	7	26.7		74.6	57	15.5	44.5	124.3	95.0	25.8		1.6484	2.0946	1.9777	1.4122
EA	y09	1	9	39.1		56.7	110	12.4	651.7	945.0	1833.3	206.7		2.8140	2.9754	3.2632	2.3153
std	std-b1-2	1	11	19.8		48.7	80.9	9.82	19.8	48.7	80.9	9.8		1.2967	1.6875	1.9079	0.9921
pha16	y21	1	13	16.8		68.1	39.2	12.8	28.0	113.5	65.3	21.3		1.4472	2.0550	1.8151	1.3291
pha15	y34	1	14	231		147	353	78.6	385.0	245.0	588.3	131.0		2.5855	2.3892	2.7696	2.1173
pha14	y45	1	15	31.5		74.9	58	16.2	52.5	124.8	96.7	27.0		1.7202	2.0963	1.9853	1.4314
pha13	y33	1	16	14.2		65	35.4	11.3	23.7	108.3	59.0	18.8		1.3741	2.0348	1.7709	1.2749
pha18	y25	1	18	248		153	358	83.7	413.3	255.0	596.7	139.5		2.6163	2.4065	2.7757	2.1446
ARM	y11	1	20	11.5		36	22.2	8.25	19.2	60.0	37.0	13.8		1.2826	1.7782	1.5682	1.1383
std	std-b1-3	1	21	21.1		47.6	82.2	9.69	21.1	47.6	82.2	9.7		1.3243	1.6776	1.9149	0.9863
std	std-b2-1	2	1	20.3		48.9	85.3	9.63	20.3	48.9	85.3	9.6		1.3075	1.6893	1.9309	0.9836
blank	y50	2	2	<0.180		<0.180	<0.530	<0.010	0.2	0.2	0.4	0.0		-0.8239	-0.8239	-0.3549	-2.0792
pha17	y16	2	3	41.1		92.8	81.7	21.6	68.5	154.7	136.2	36.0		1.8357	2.1894	2.1341	1.5563
ARM	y42	2	4	11		36.9	23.4	8.79	18.3	61.5	39.0	14.7		1.2633	1.7889	1.5911	1.1658
pha13	y39	2	5	14		70.6	37.1	11.2	23.3	117.7	61.8	18.7		1.3680	2.0707	1.7912	1.2711
pha15	y24	2	10	240		154	362	75.3	400.0	256.7	603.3	125.5		2.6021	2.4094	2.7806	2.0987
std	std-b2-2	2	11	22.4		48.8	83.2	9.5	22.4	48.8	83.2	9.5		1.3502	1.6884	1.9201	0.9777
pha18	y10	2	13	244		162	385	80.1	406.7	270.0	641.7	133.5		2.6092	2.4314	2.8073	2.1255
pha14	y23	2	14	30.4		77	59	15.2	50.7	128.3	98.3	25.3		1.7047	2.1083	1.9927	1.4037
EA	y46	2	17	41.2		56.1	107	11.6	686.7	935.0	1783.3	193.3		2.8367	2.9708	3.2512	2.2863
pha16	y32	2	20	17.5		71.9	41.3	12.3	29.2	119.8	68.8	20.5		1.4649	2.0786	1.8378	1.3118
std	std-b2-3	2	21	20.5		47.6	85	9.12	20.5	47.6	85.0	9.1		1.3118	1.6776	1.9294	0.9600
std	std-b3-1	3	1	20.1		50.4	86.4	10.6	20.1	50.4	86.4	10.6		1.3032	1.7024	1.9365	1.0253
pha16	y19	3	2	16.8		69.2	39.1	12	28.0	115.3	65.2	20.0		1.4472	2.0620	1.8140	1.3010
EA	y03	3	4	38.1		55.6	116	13.4	635.0	926.7	1933.3	223.3		2.8028	2.9669	3.2863	2.3490
pha14	y49	3	7	26		75.1	55.2	15.2	43.3	125.2	92.0	25.3		1.6368	2.0975	1.9638	1.4037
pha17	y04	3	8	37.6		92	79.8	21.7	62.7	153.3	133.0	36.2		1.7970	2.1856	2.1239	1.5583
std	std-b3-2	3	9	20.2		48.1	84.4	10.3	20.2	48.1	84.4	10.3		1.3054	1.6821	1.9263	1.0128
ARM	y27	3	11	11.3		36	23.8	9.26	18.8	60.0	39.7	15.4		1.2749	1.7782	1.5984	1.1885
pha13	y02	3	14	13.9		65.6	36.4	11.9	23.2	109.3	60.7	19.8		1.3649	2.0388	1.7830	1.2974
pha18	y13	3	15	246		168	376	88.5	410.0	280.0	626.7	147.5		2.6128	2.4472	2.7970	2.1688
pha15	y26	3	16	239		146	360	80.5	398.3	243.3	600.0	134.2		2.6003	2.3862	2.7782	2.1277
std	std-b3-3	3	17	22.2		47.5	82.3	9.94	22.2	47.5	82.3	9.9		1.3464	1.6767	1.9154	0.9974

Notes:

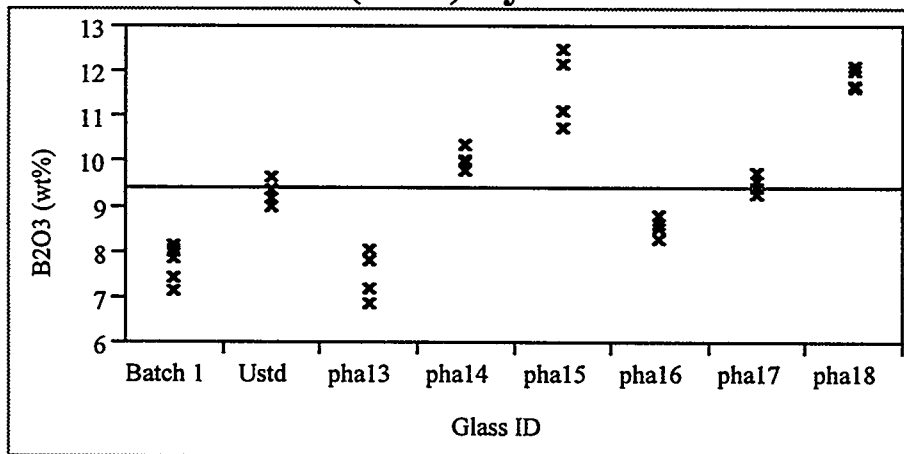
- (1). Values that are below detection (indicated by a "<") were converted to ½ the detection limit.
- (2) The CST Phase 2 and kgb glasses were also analyzed with these data but their values are not shown in this table. See [5] for a complete listing of the data.

Exhibit A.1: Measurements by Glass Sample ID by Oxide

Al₂O₃ (wt%) By Glass ID



B₂O₃ (wt%) By Glass ID



CaO MW (wt%) By Glass ID

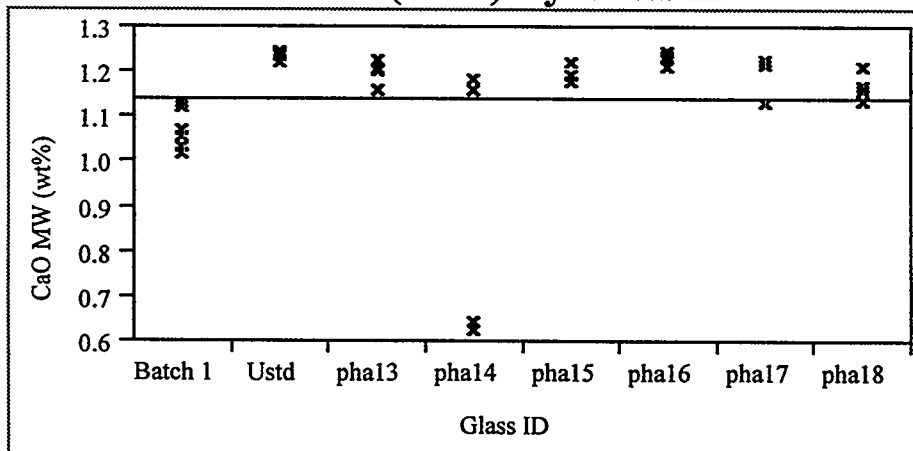
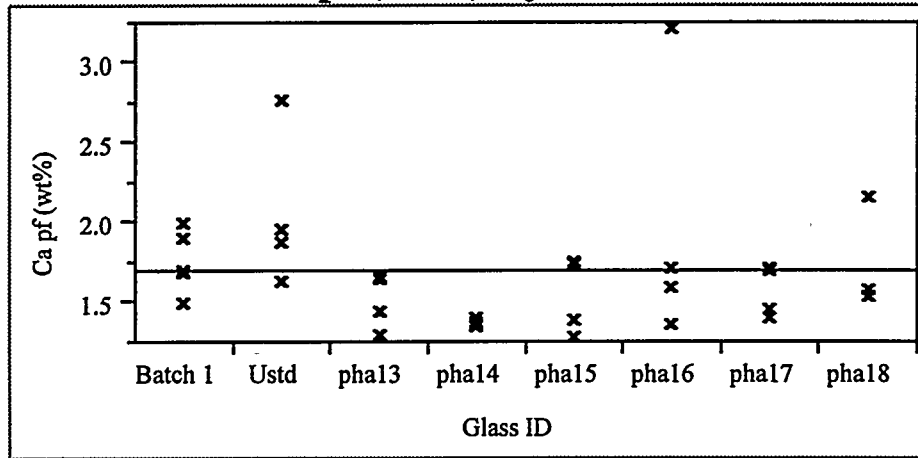
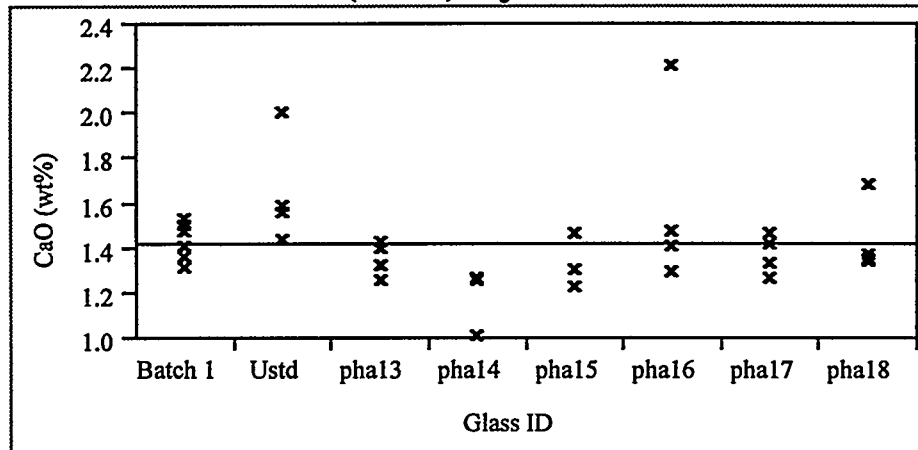


**Exhibit A.1: Measurements by Glass Sample ID by Oxide
(continued)**

CaO pf (wt%) By Glass ID



CaO (wt%) By Glass ID



Cr2O3 (wt%) By Glass ID

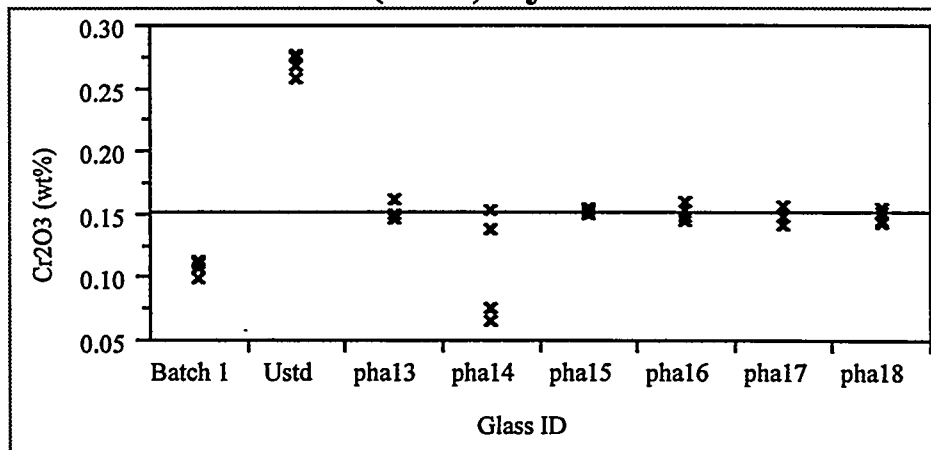
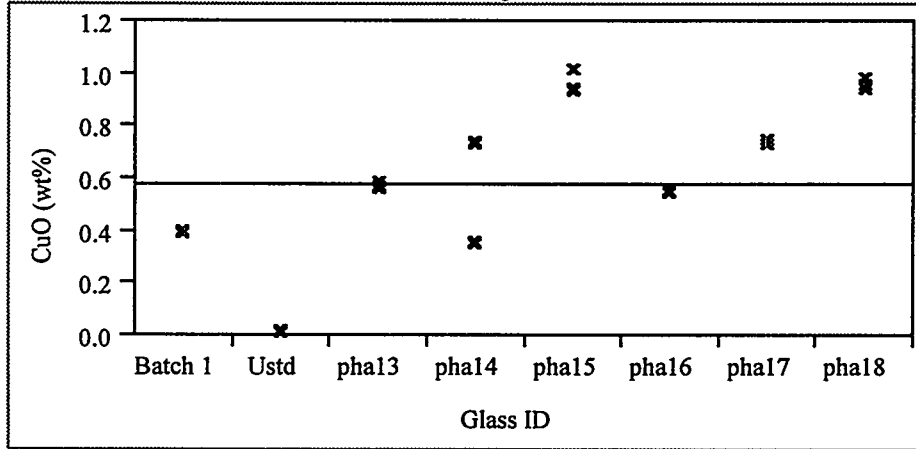
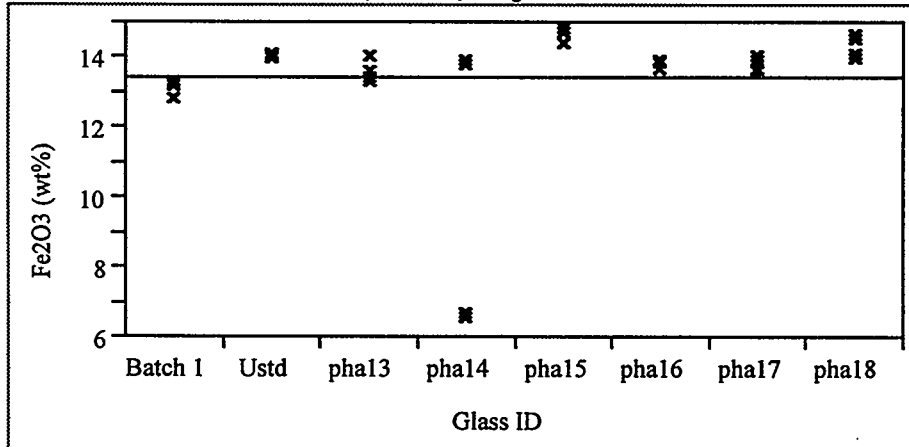


Exhibit A.1: Measurements by Glass Sample ID by Oxide
(continued)

CuO (wt%) By Glass ID



Fe2O3 (wt%) By Glass ID



K2O (wt%) By Glass ID

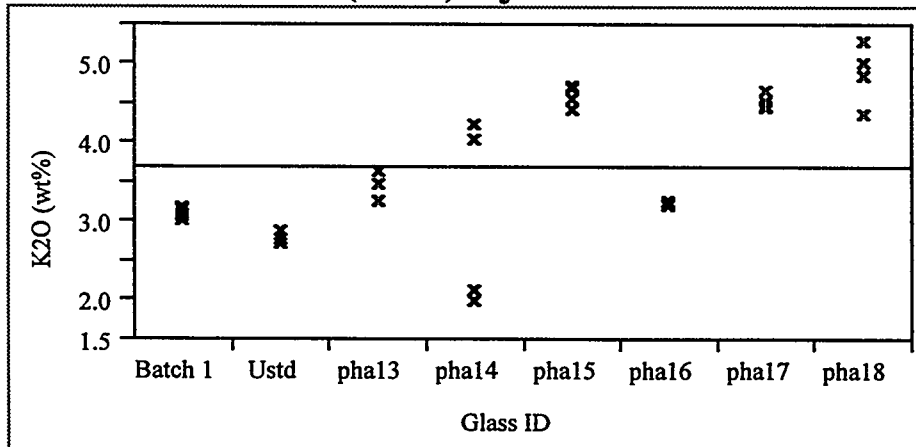
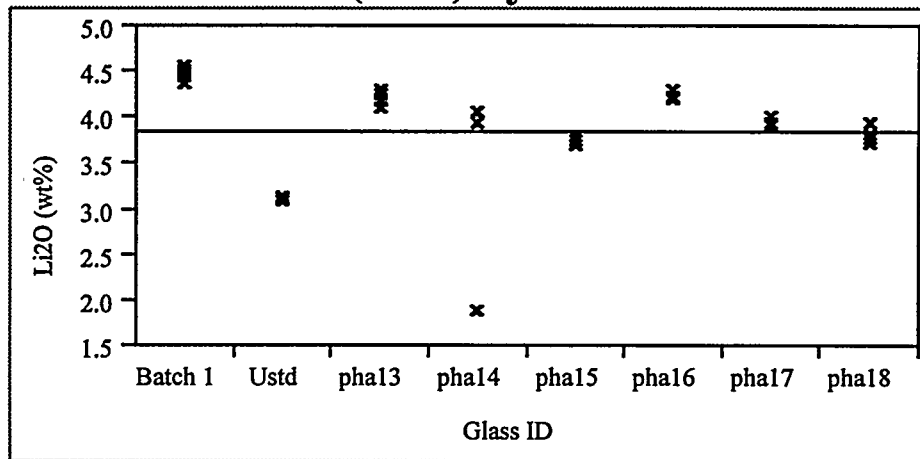
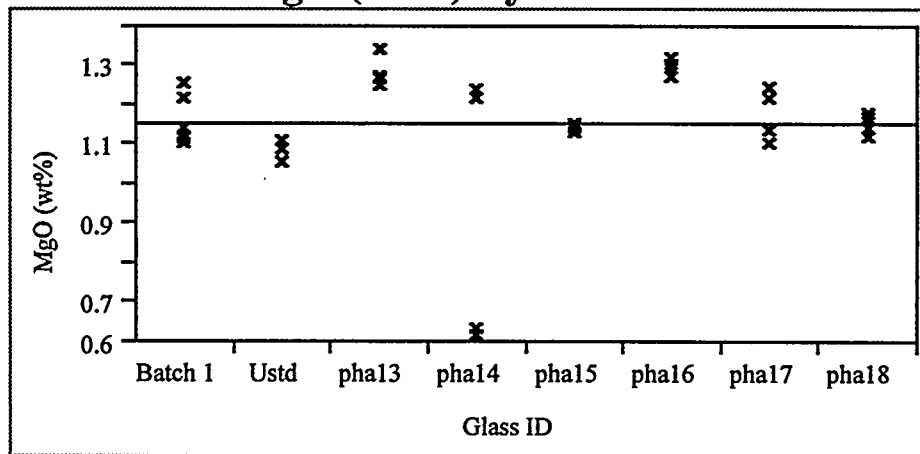


**Exhibit A.1: Measurements by Glass Sample ID by Oxide
(continued)**

Li₂O (wt%) By Glass ID



MgO (wt%) By Glass ID



MnO (wt%) By Glass ID

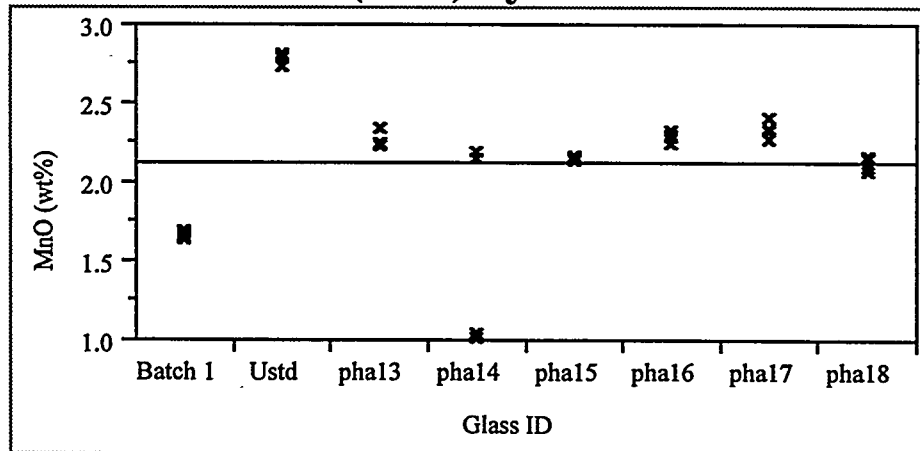
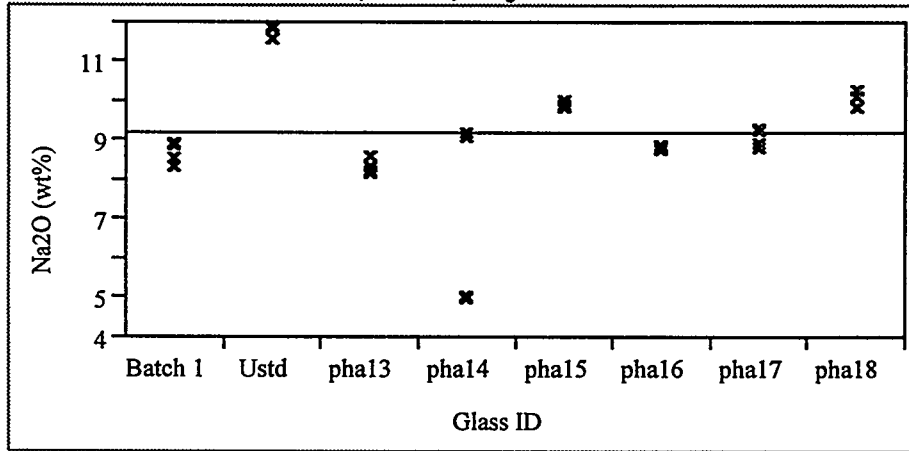
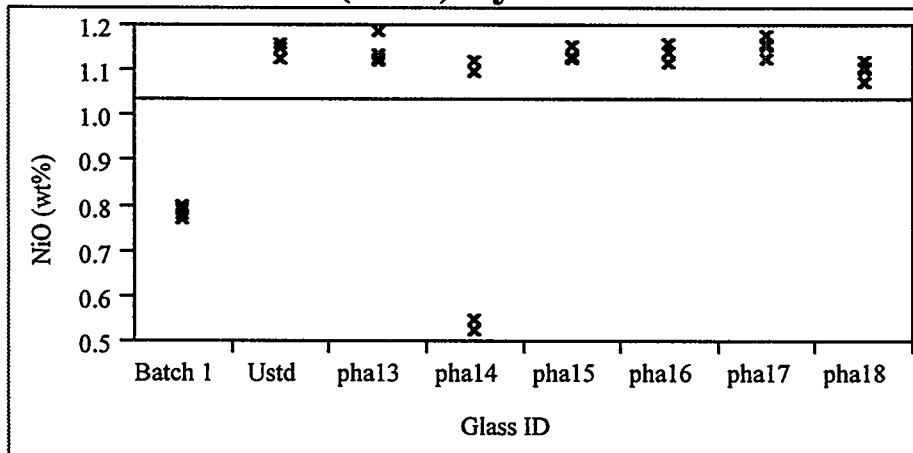


Exhibit A.1: Measurements by Glass Sample ID by Oxide
(continued)

Na₂O (wt%) By Glass ID



NiO (wt%) By Glass ID



SiO₂ MW (wt%) By Glass ID

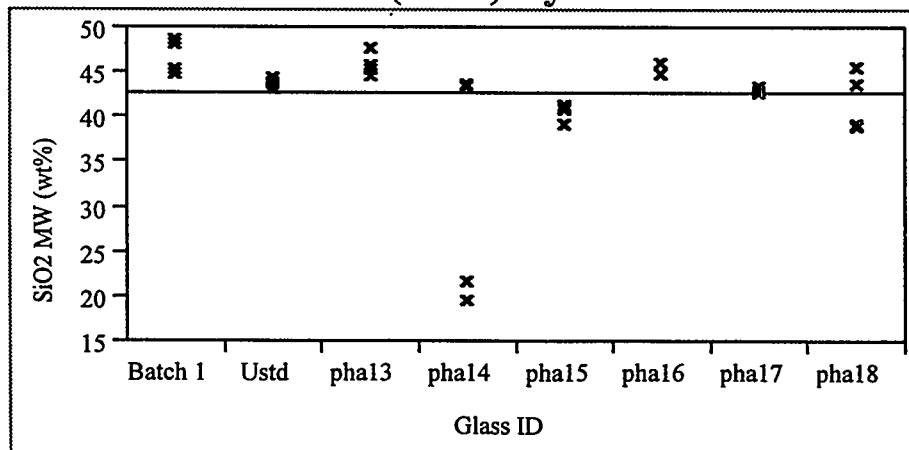
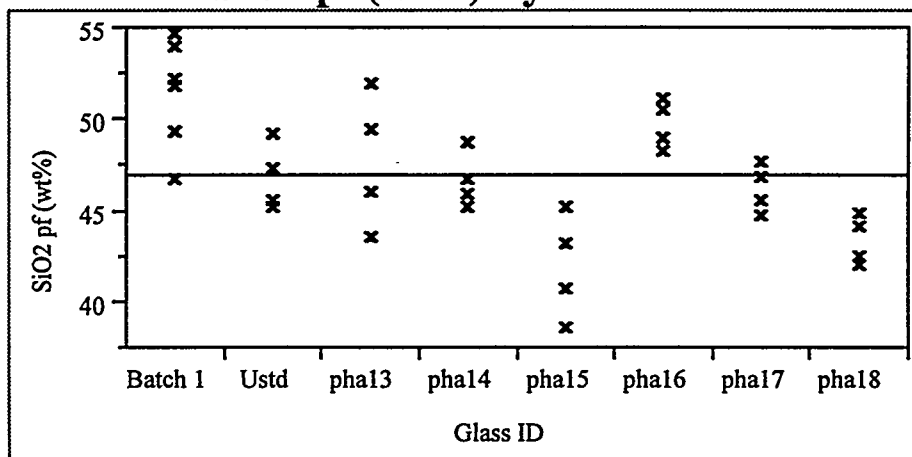
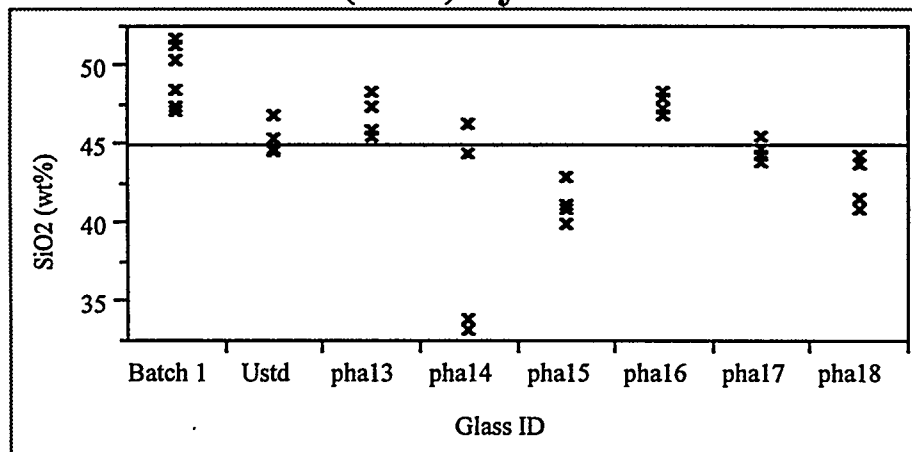


Exhibit A.1: Measurements by Glass Sample ID by Oxide
(continued)

SiO₂ pf (wt%) By Glass ID



SiO₂ (wt%) By Glass ID



TiO₂ (wt%) By Glass ID

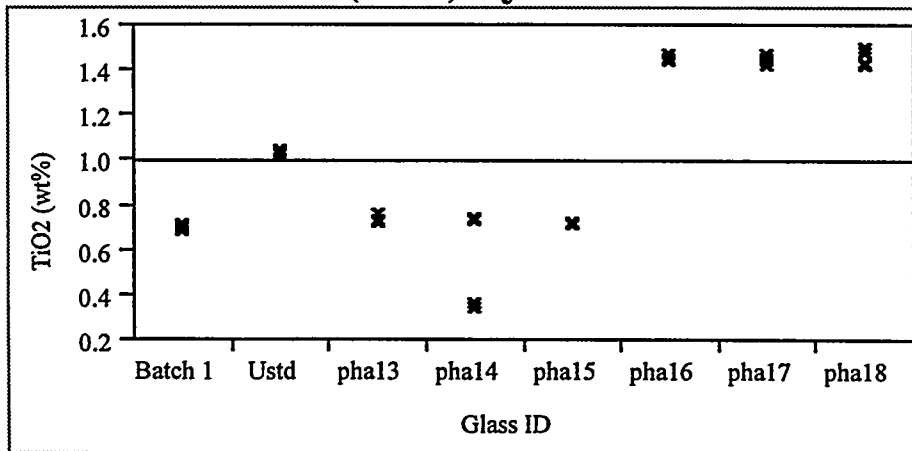
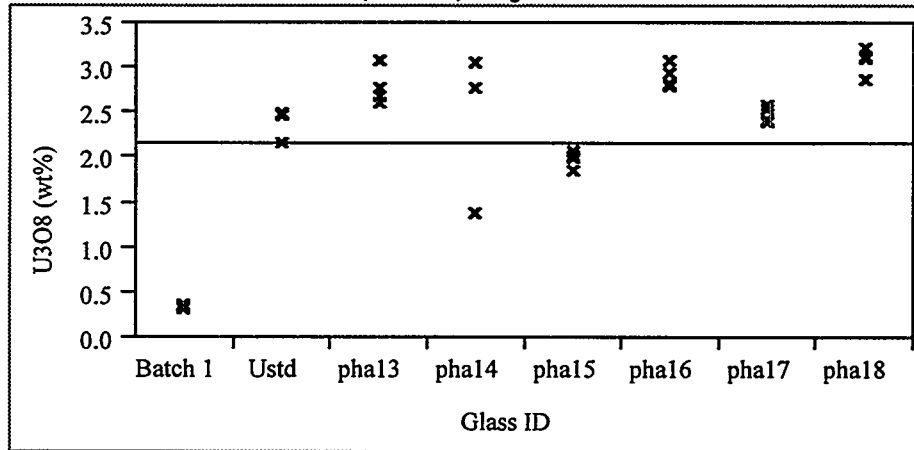
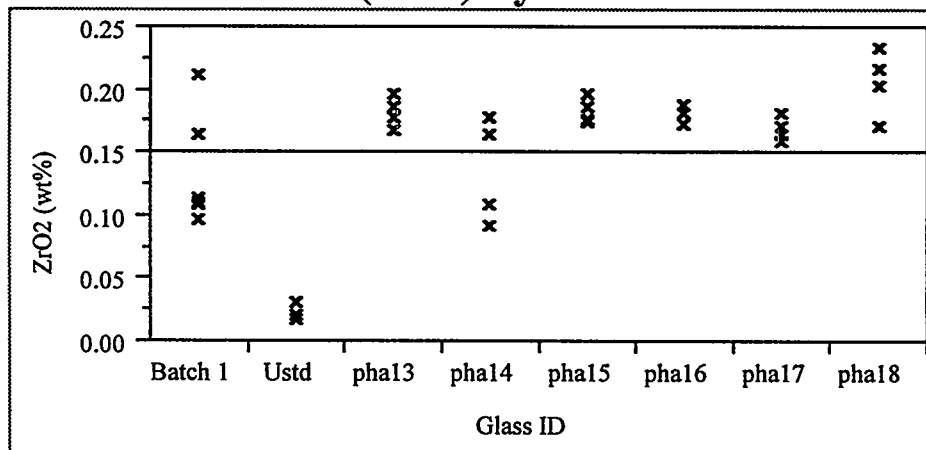


Exhibit A.1: Measurements by Glass Sample ID by Oxide
(continued)

U3O8 (wt%) By Glass ID



ZrO2 (wt%) By Glass ID



Sum of Oxides (m) By Glass ID

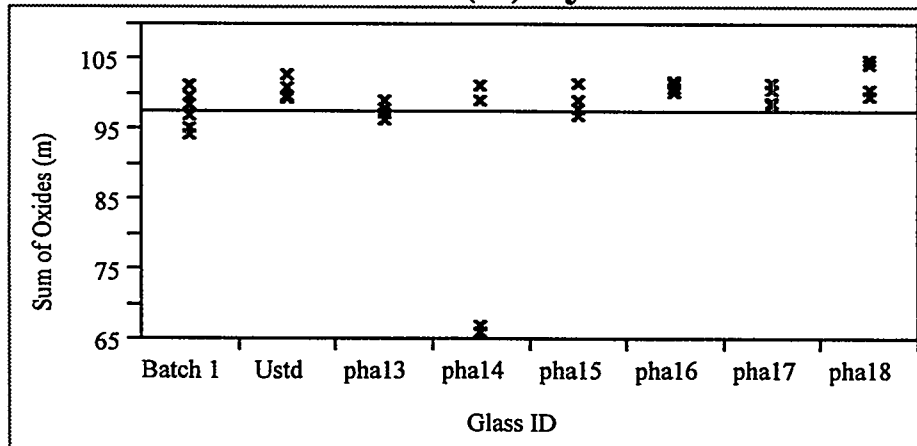


Exhibit A.2: Peroxide Fusion Measurements of Glass Standards by Oxide
(+ Ustd; small square Batch 1 standard)

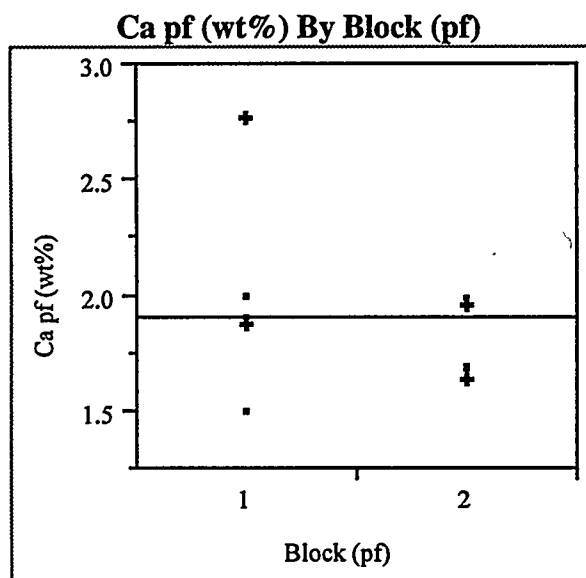
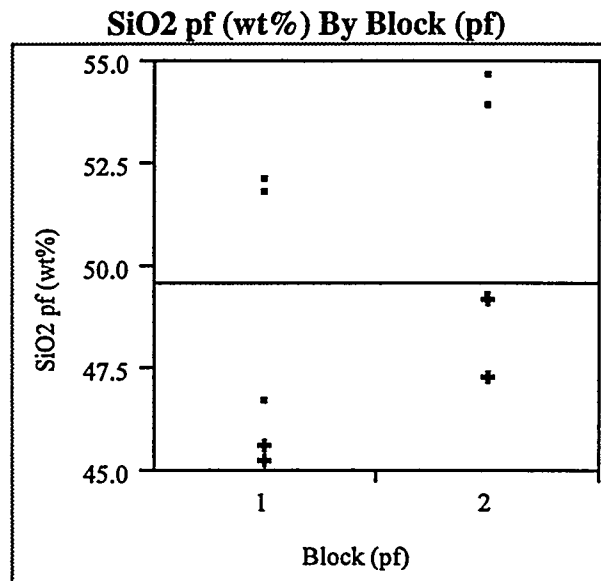
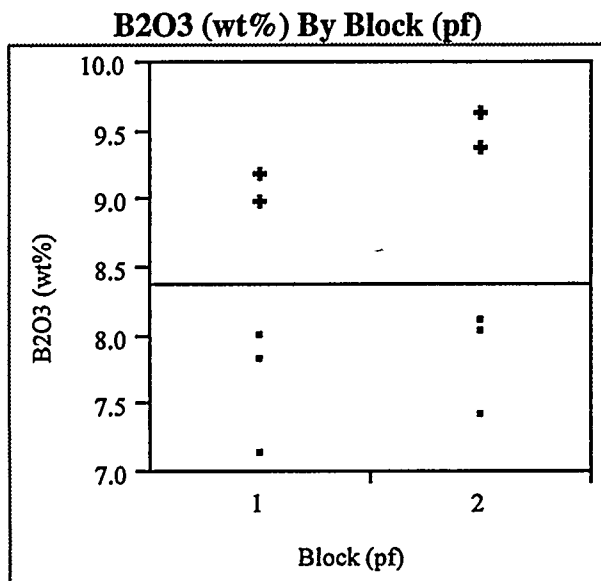
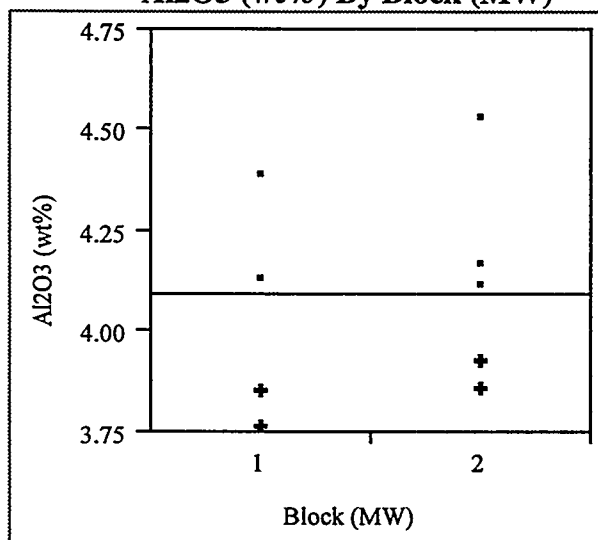
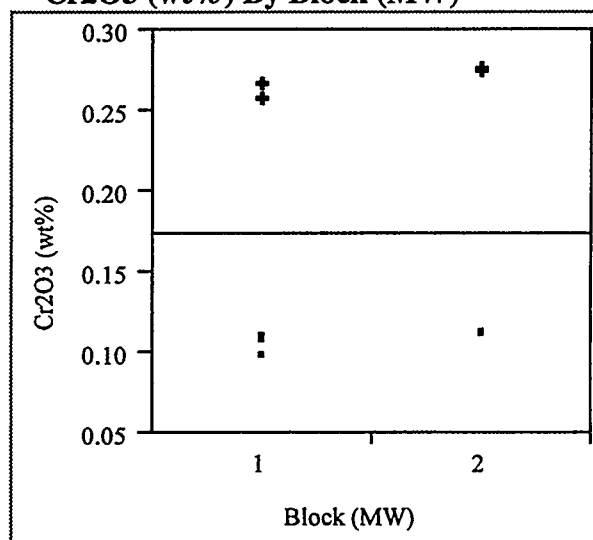


Exhibit A.3: Microwave Measurements of Glass Standards by Oxide
(+ Ustd; small square Batch 1 standard)

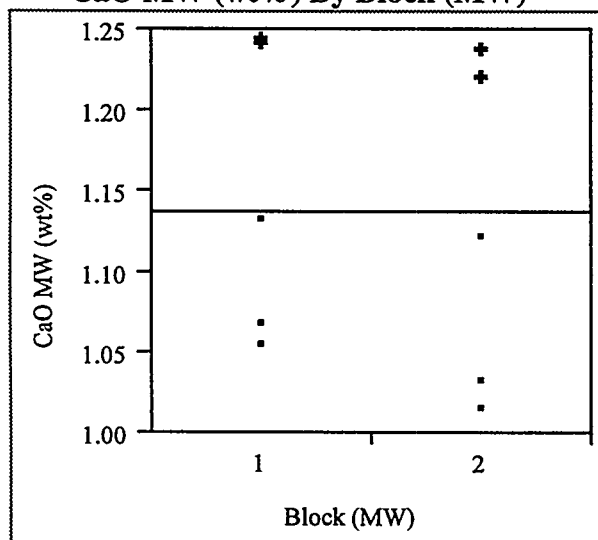
Al₂O₃ (wt%) By Block (MW)



Cr₂O₃ (wt%) By Block (MW)



CaO MW (wt%) By Block (MW)



CuO (wt%) By Block (MW)

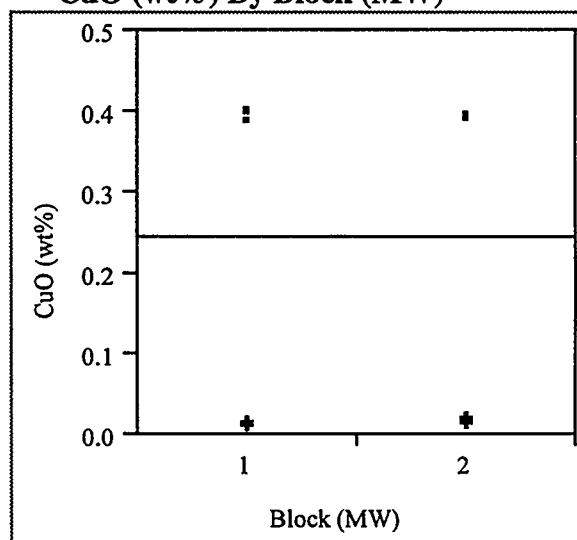
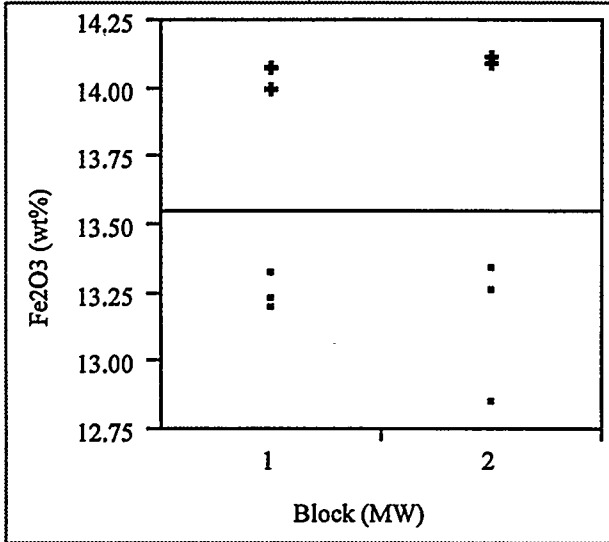
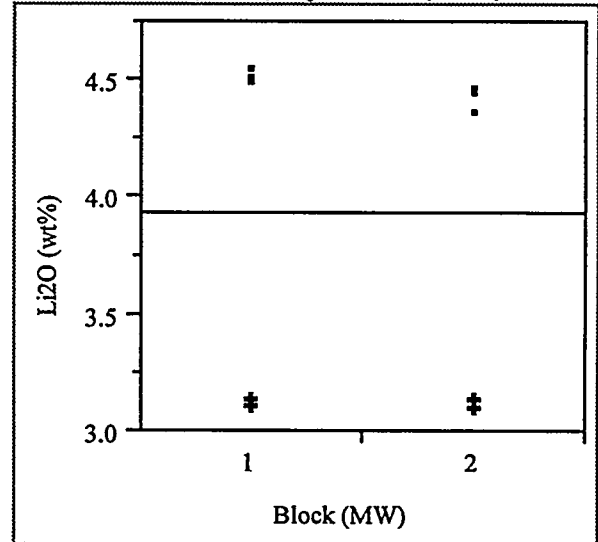


Exhibit A.3: Microwave Measurements of Glass Standards by Oxide
 (+ Ustd; small square Batch 1 standard)
 (continued)

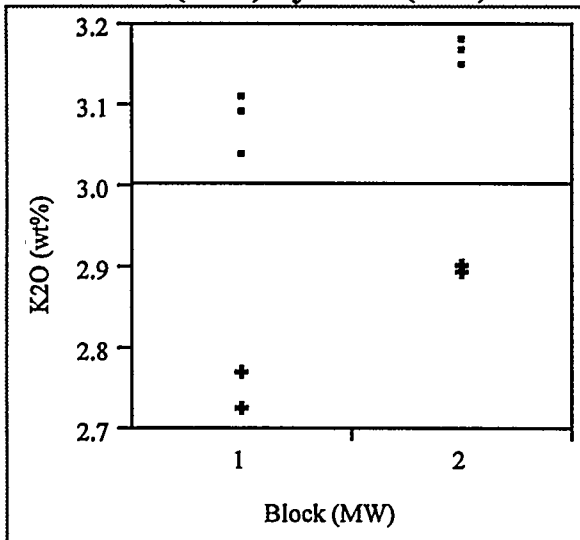
Fe₂O₃ (wt%) By Block (MW)



Li₂O (wt%) By Block (MW)



K₂O (wt%) By Block (MW)



MgO (wt%) By Block (MW)

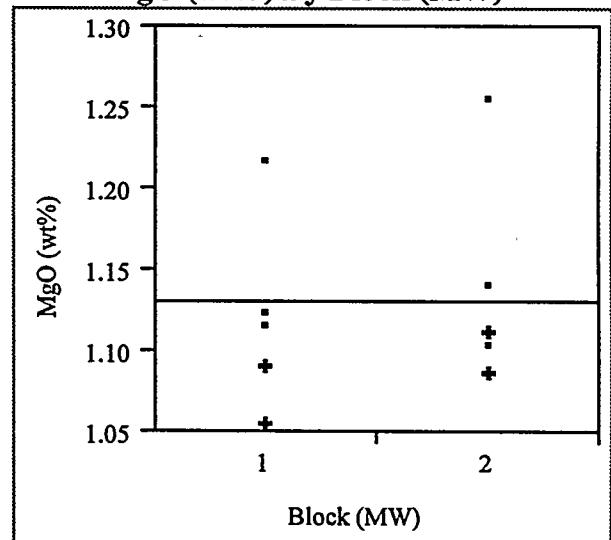
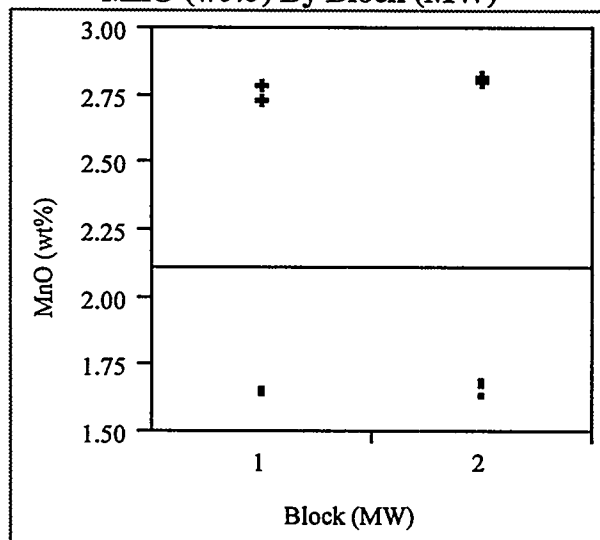
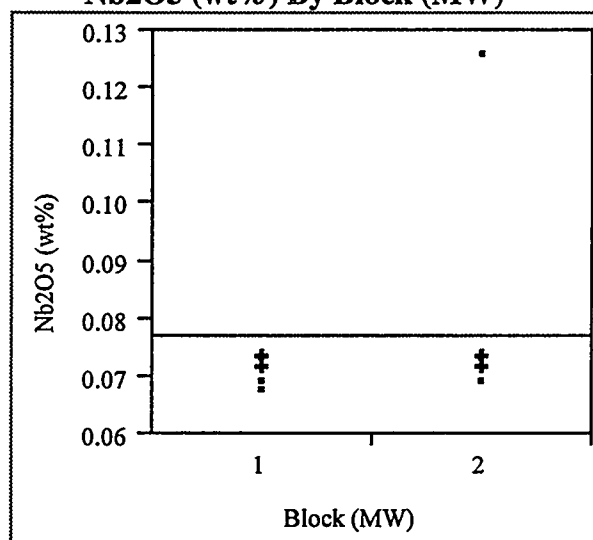


Exhibit A.3: Microwave Measurements of Glass Standards by Oxide
(+ Ustd; small square Batch 1 standard)
(continued)

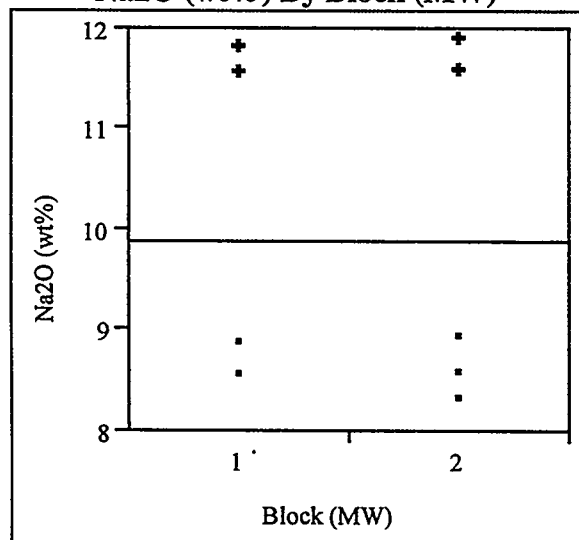
MnO (wt%) By Block (MW)



Nb2O5 (wt%) By Block (MW)



Na2O (wt%) By Block (MW)



NiO (wt%) By Block (MW)

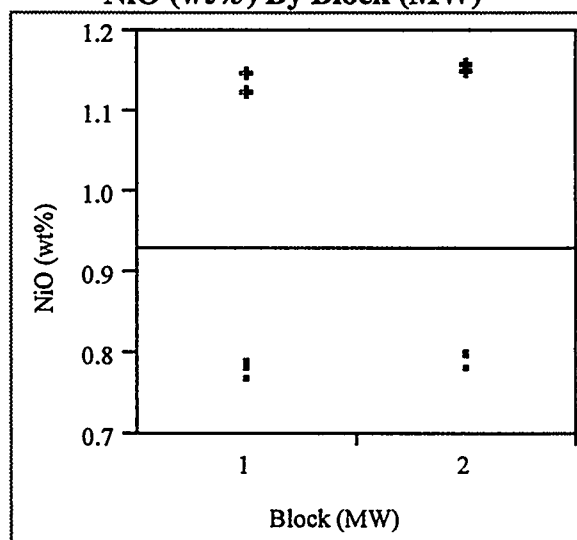
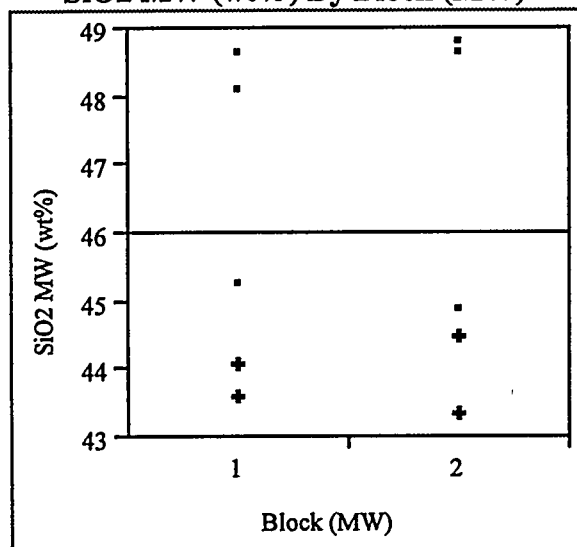
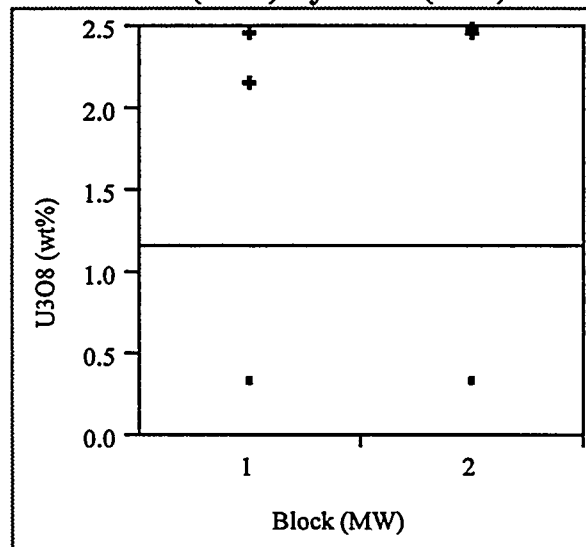


Exhibit A.3: Microwave Measurements of Glass Standards by Oxide
(+ Ustd; small square Batch 1 standard)
(continued)

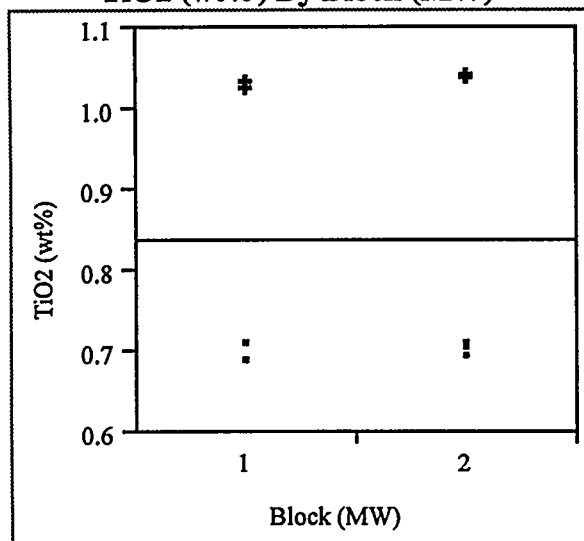
SiO₂ MW (wt%) By Block (MW)



U₃O₈ (wt%) By Block (MW)



TiO₂ (wt%) By Block (MW)



ZrO₂ (wt%) By Block (MW)

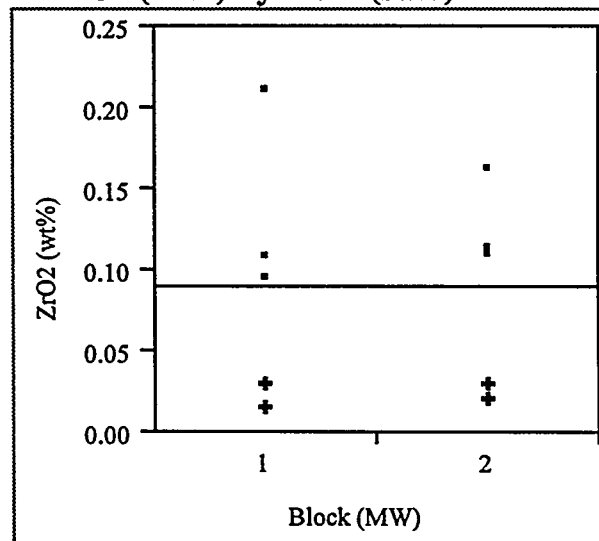


Exhibit A.4: Comparisons of Measurements versus Target Compositions
(concentrations in weight percents)

Al₂O₃

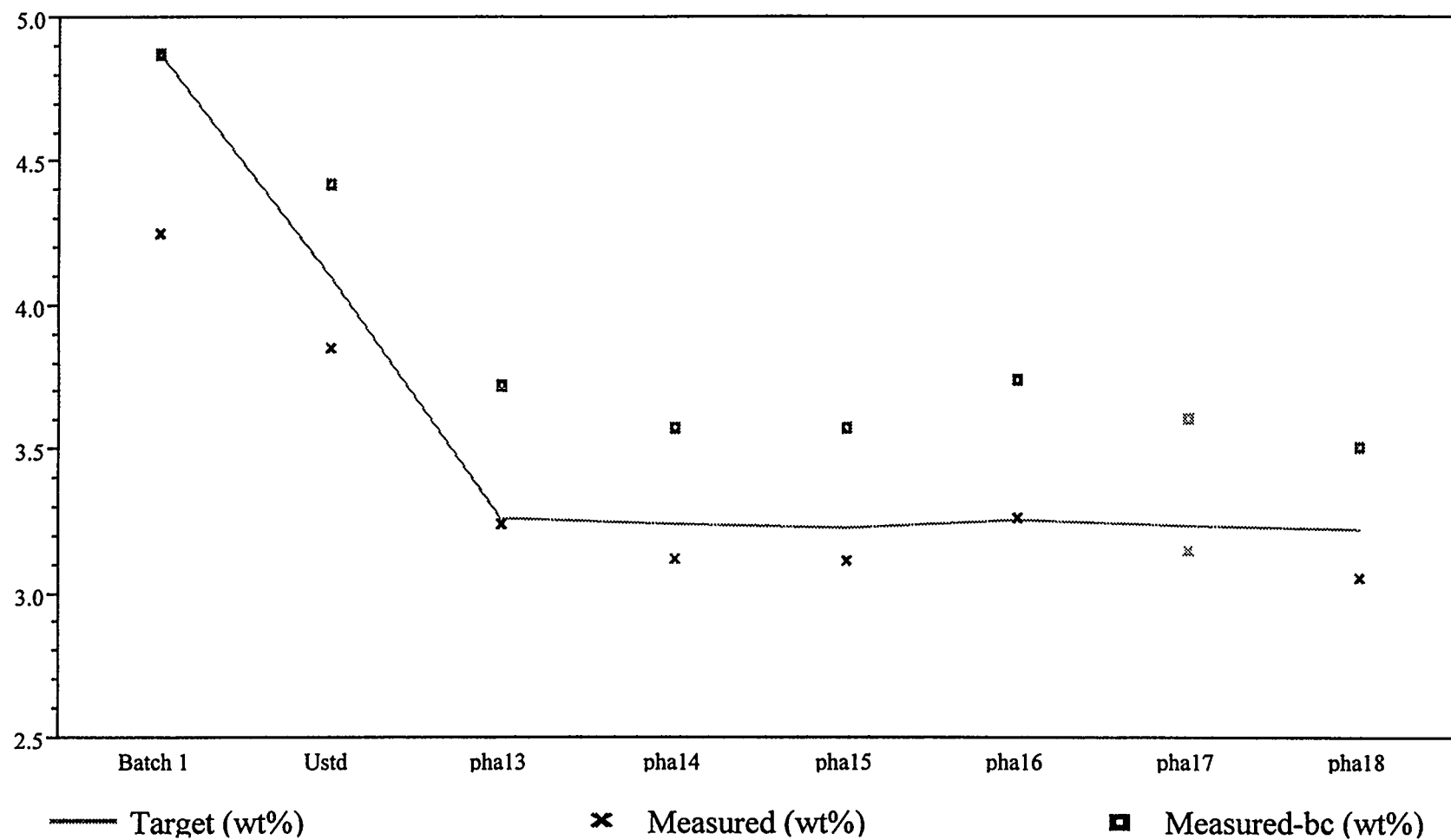


Exhibit A.4: Comparisons of Measurements versus Target Compositions
(concentrations in weight percents)

B2O3

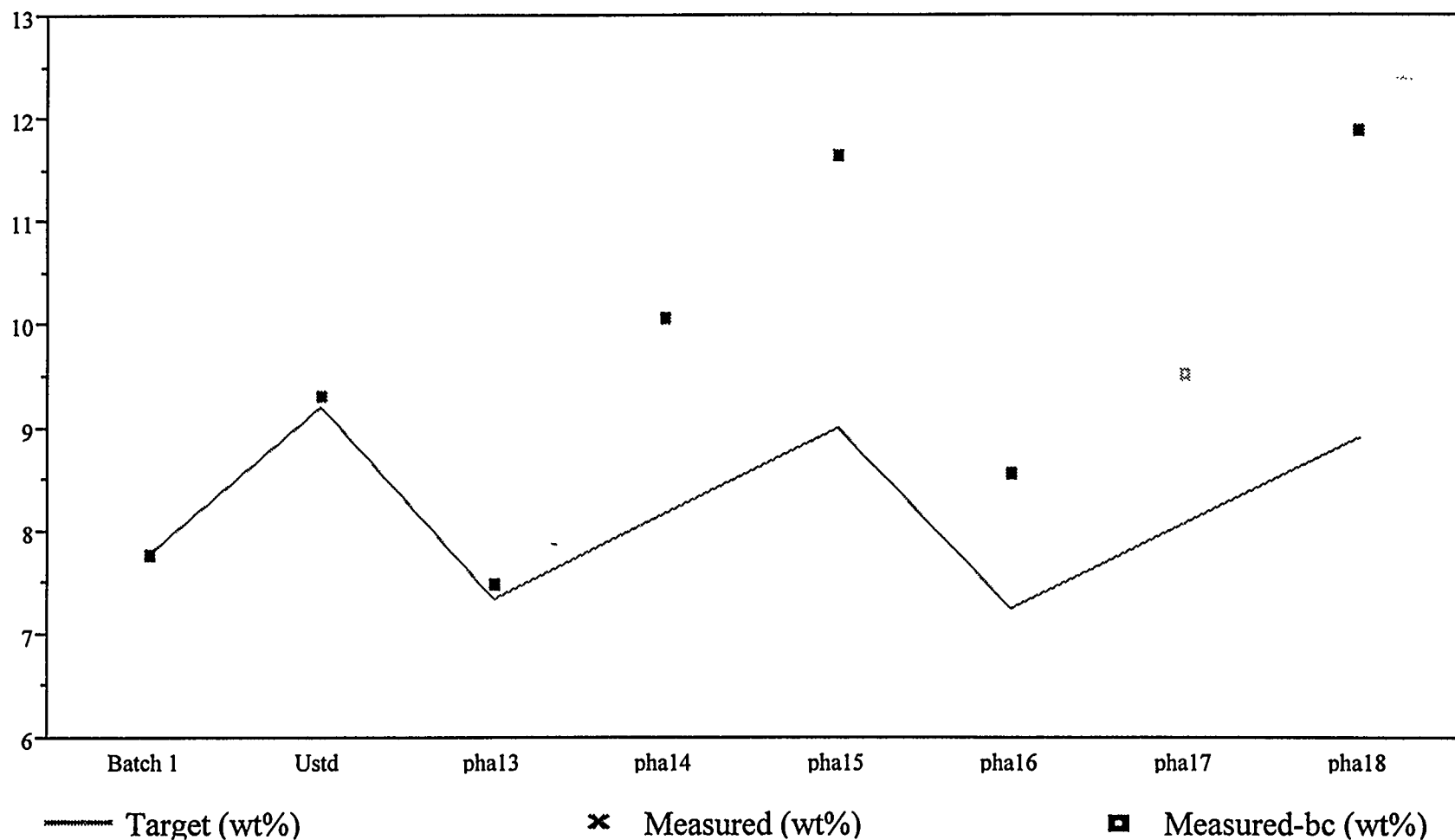


Exhibit A.4: Comparisons of Measurements versus Target Compositions
(concentrations in weight percents)

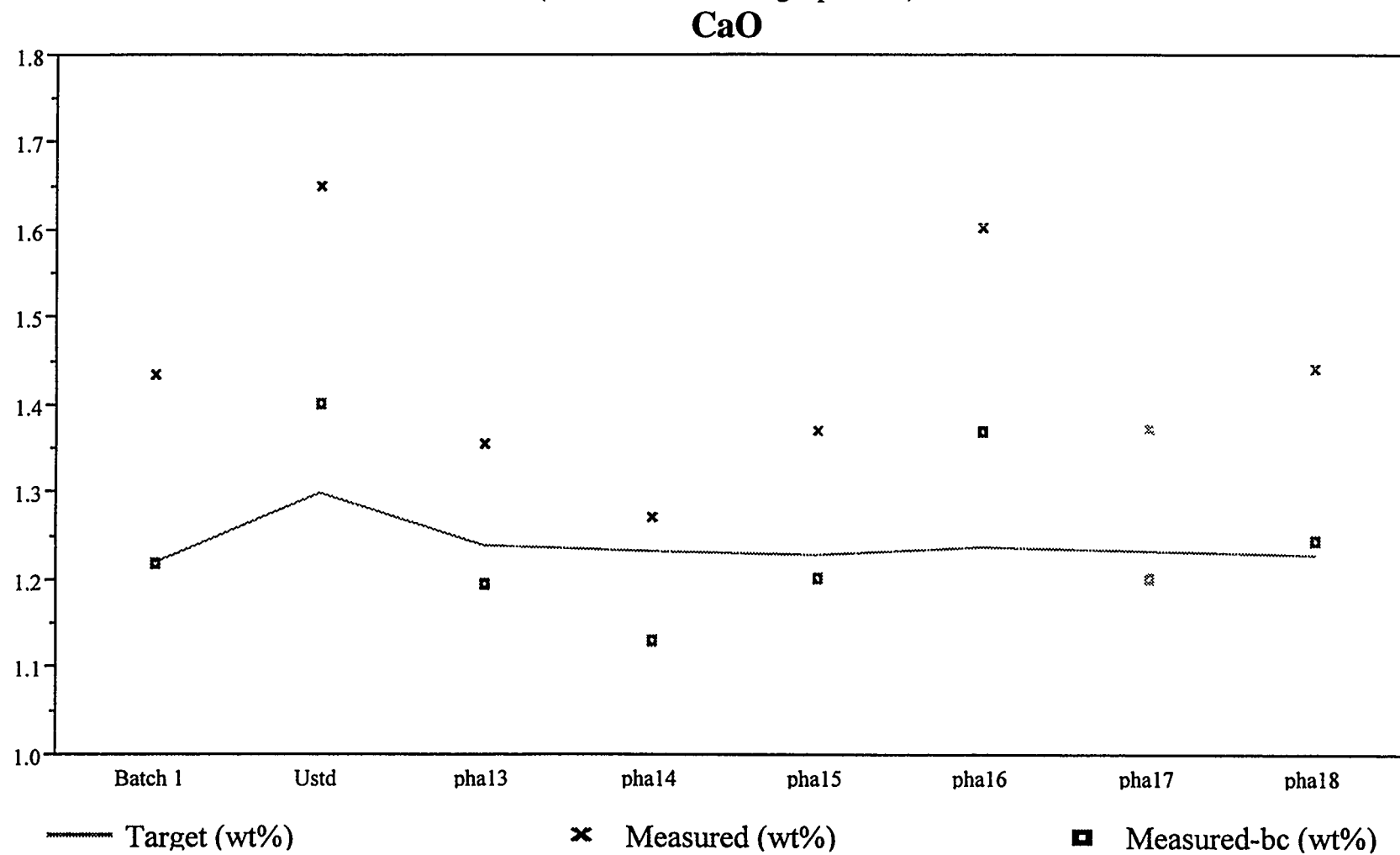


Exhibit A.4: Comparisons of Measurements versus Target Compositions
(concentrations in weight percents)

Cr₂O₃

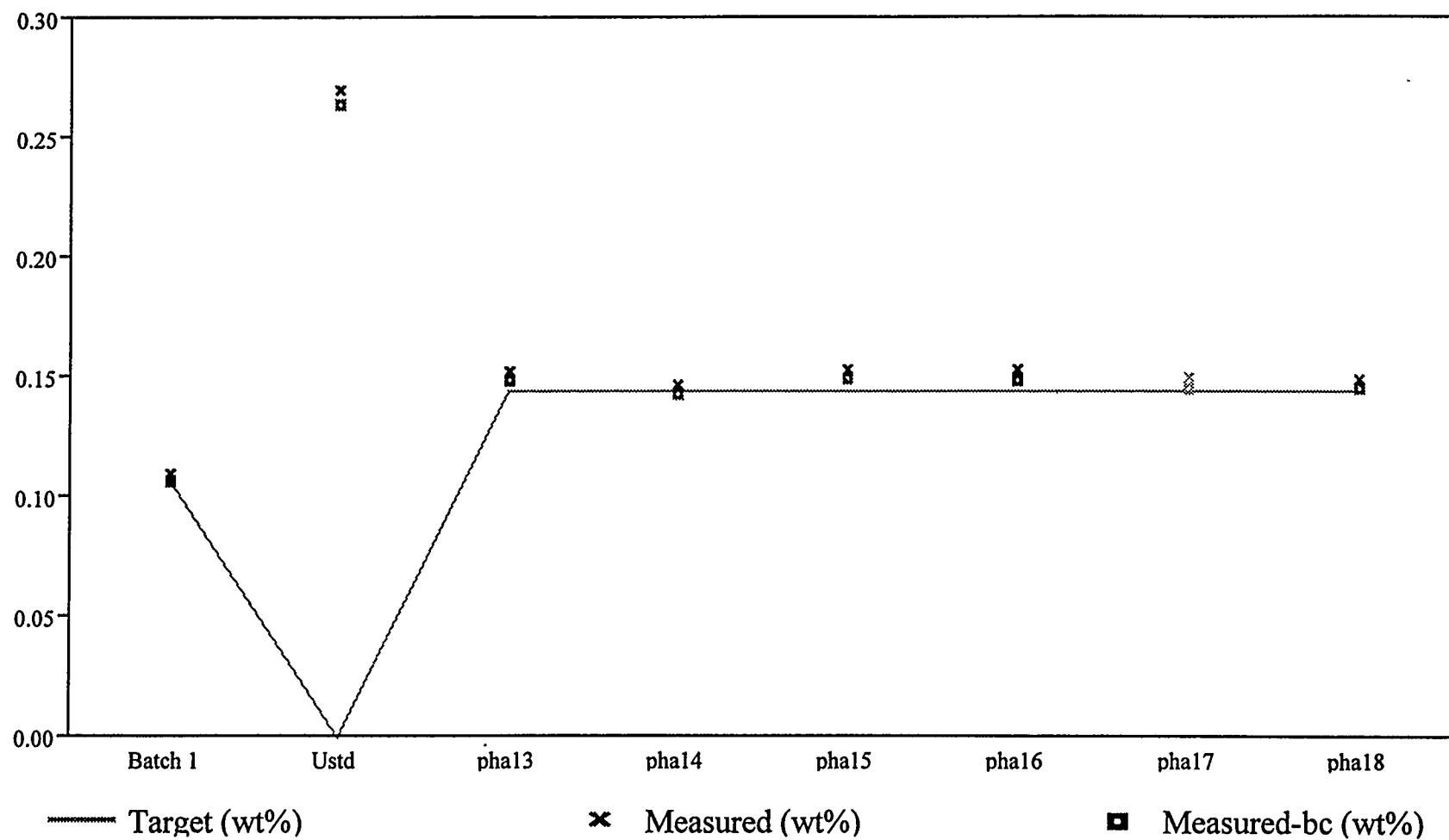


Exhibit A.4: Comparisons of Measurements versus Target Compositions
(concentrations in weight percents)

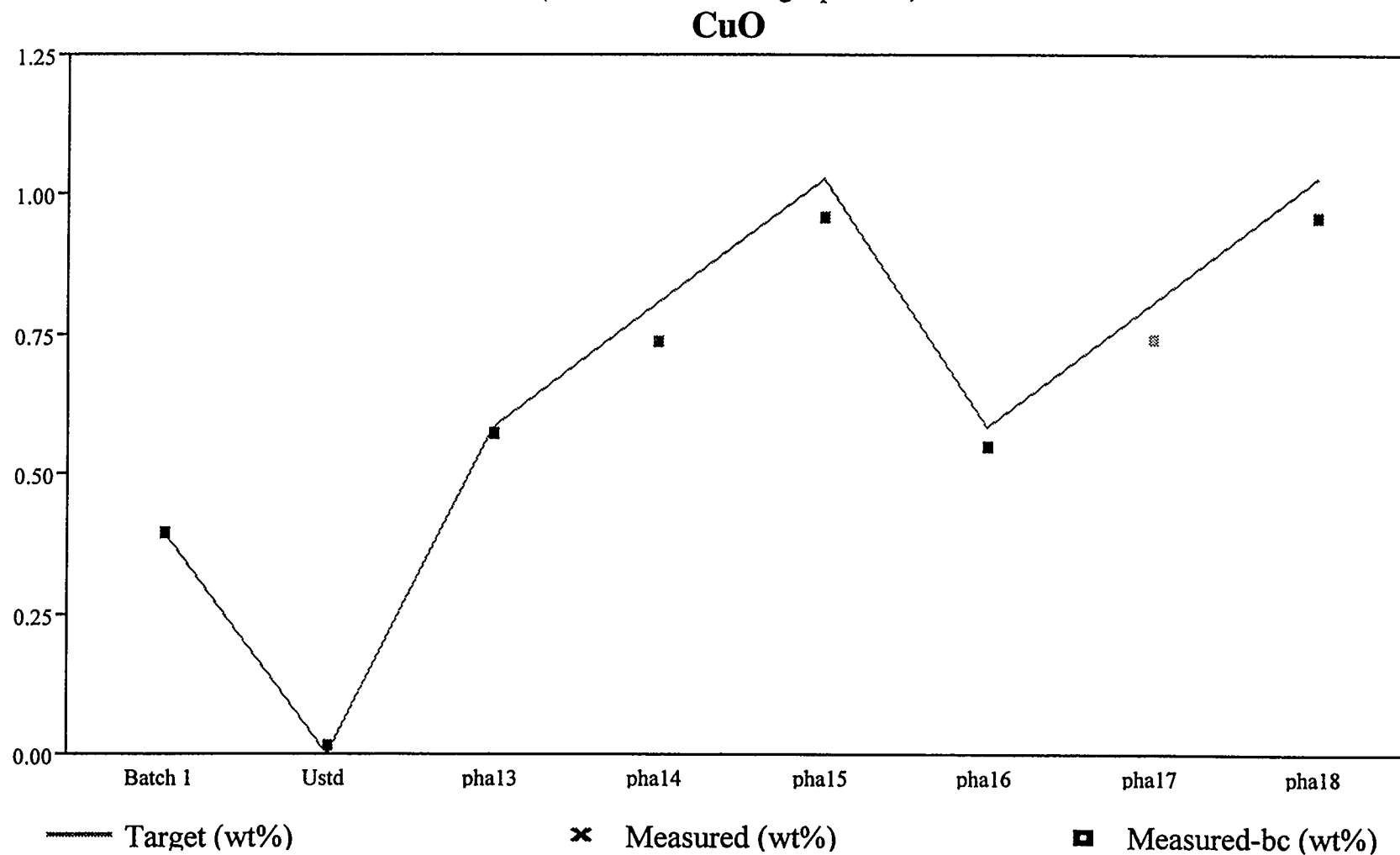


Exhibit A.4: Comparisons of Measurements versus Target Compositions
(concentrations in weight percents)

Fe₂O₃

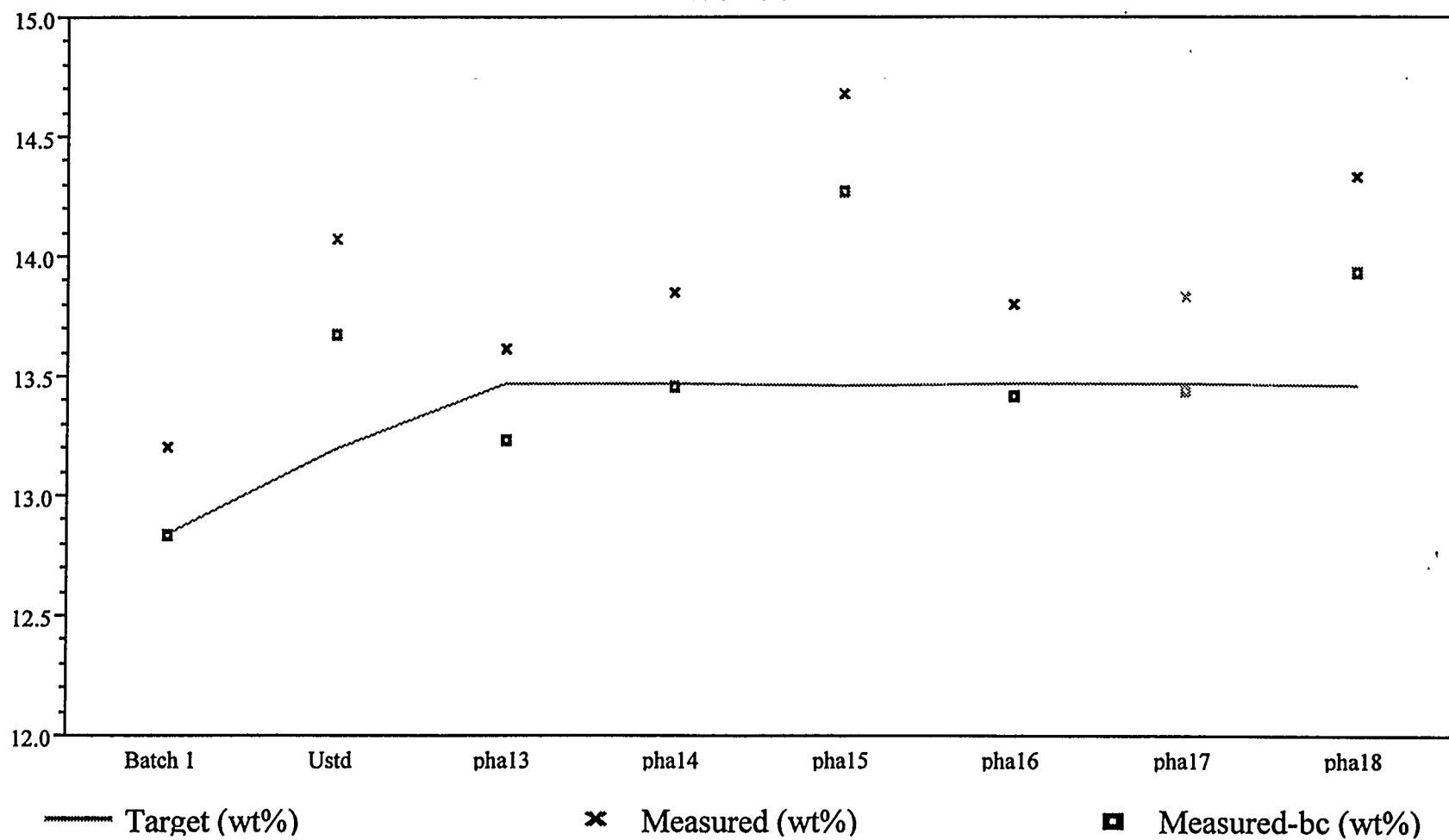


Exhibit A.4: Comparisons of Measurements versus Target Compositions
(concentrations in weight percents)

K₂O

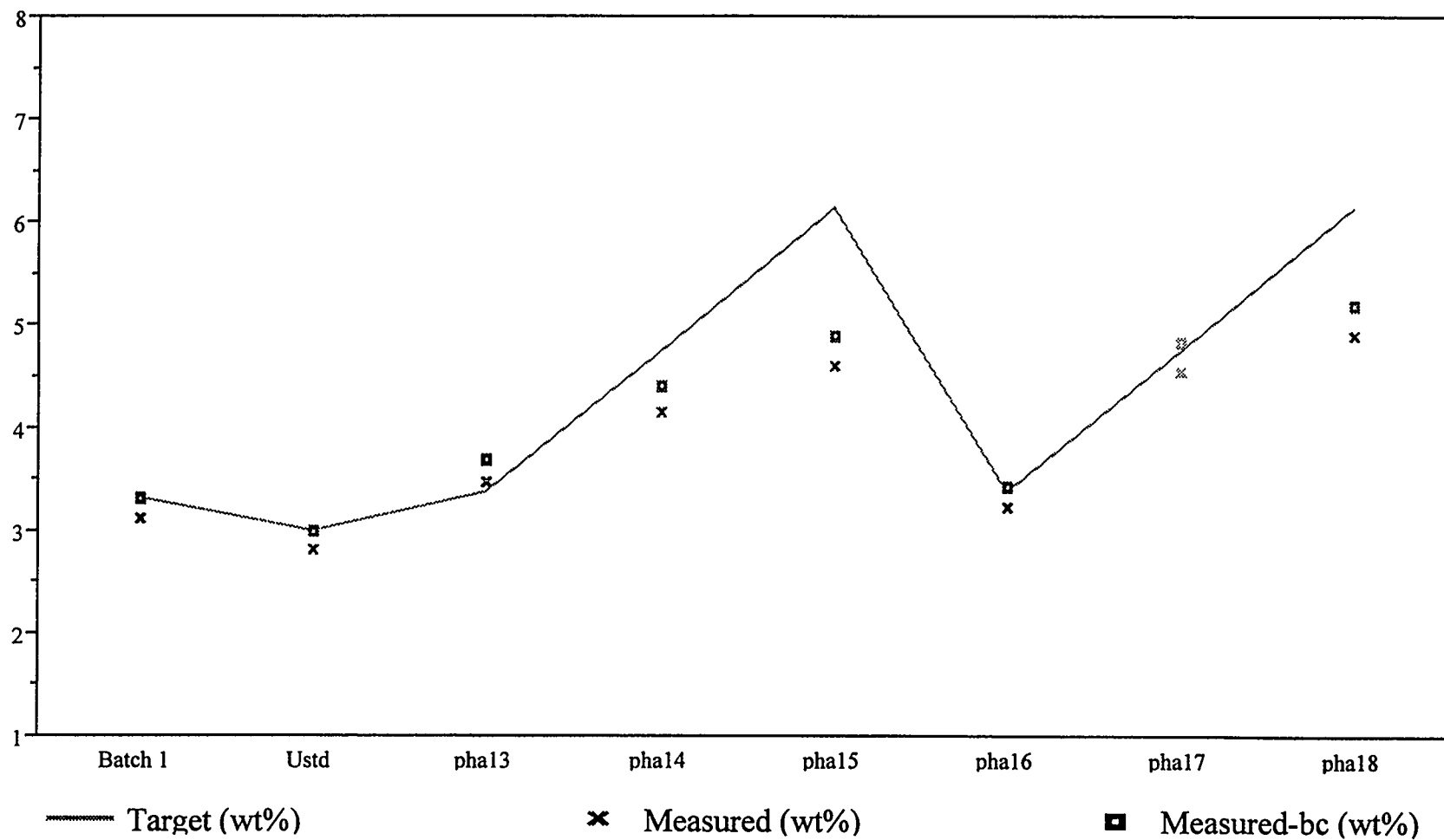


Exhibit A.4: Comparisons of Measurements versus Target Compositions
(concentrations in weight percents)

Li2O

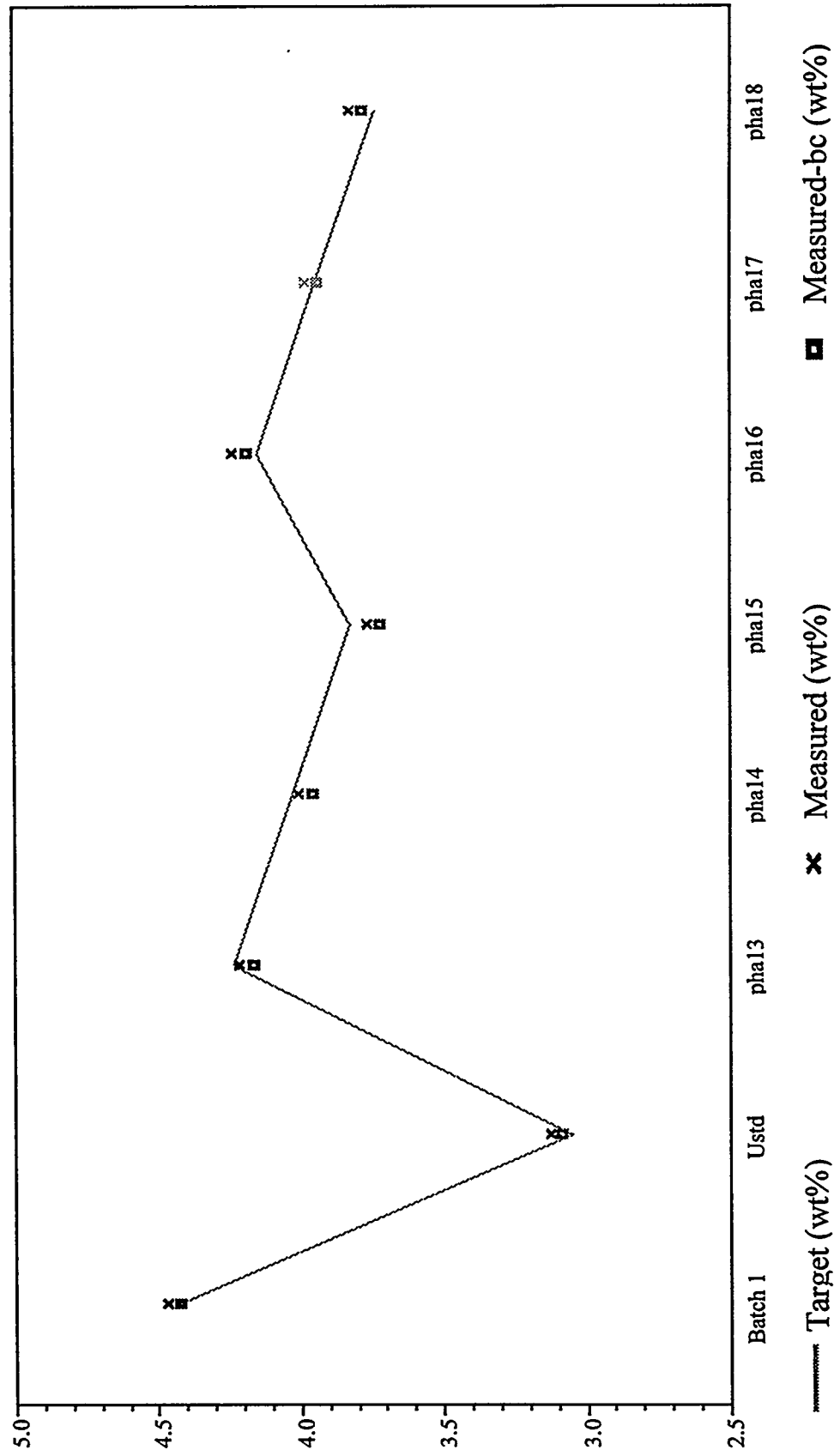


Exhibit A.4: Comparisons of Measurements versus Target Compositions
(concentrations in weight percents)

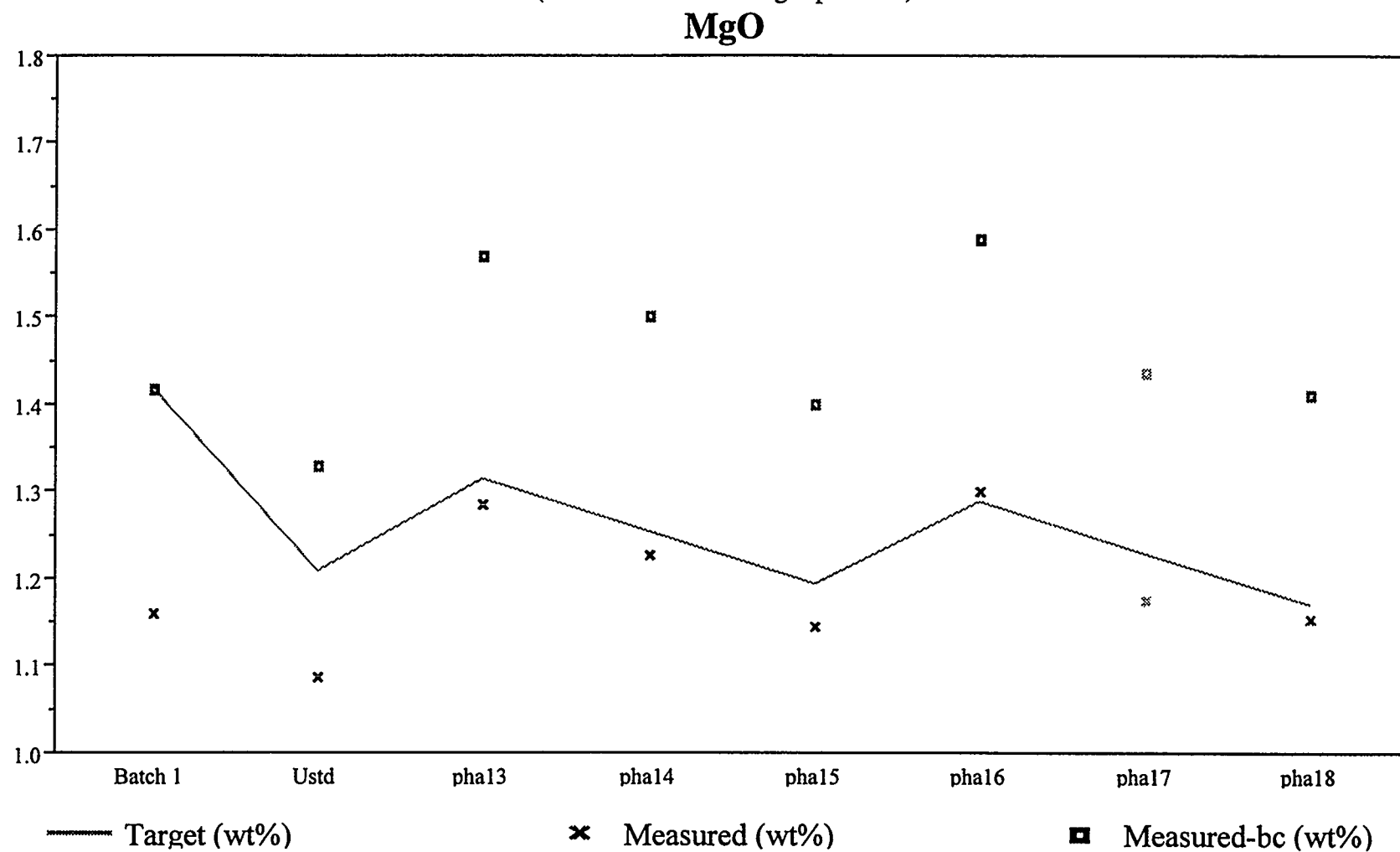


Exhibit A.4: Comparisons of Measurements versus Target Compositions
(concentrations in weight percents)

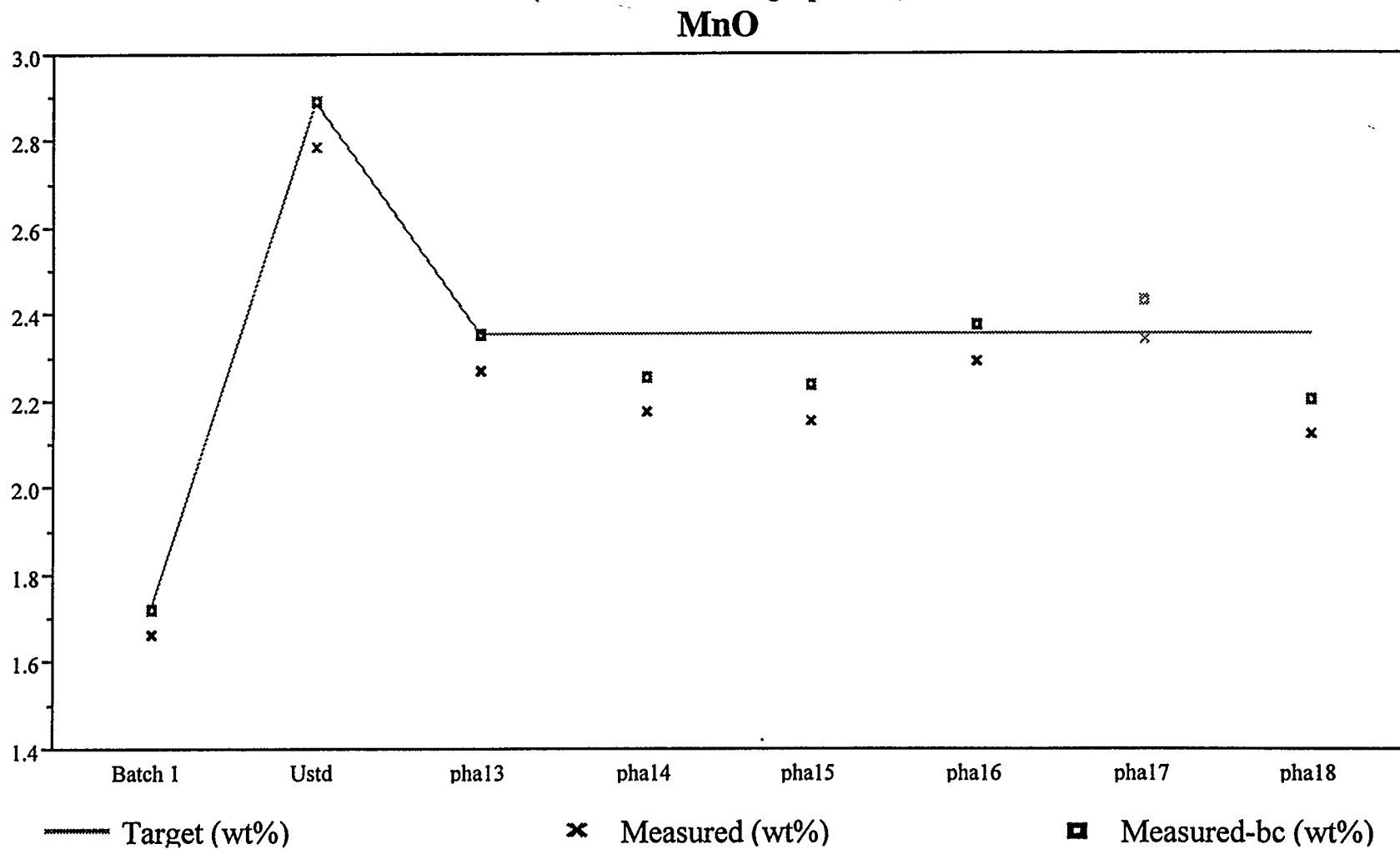


Exhibit A.4: Comparisons of Measurements versus Target Compositions
(concentrations in weight percents)

Na₂O

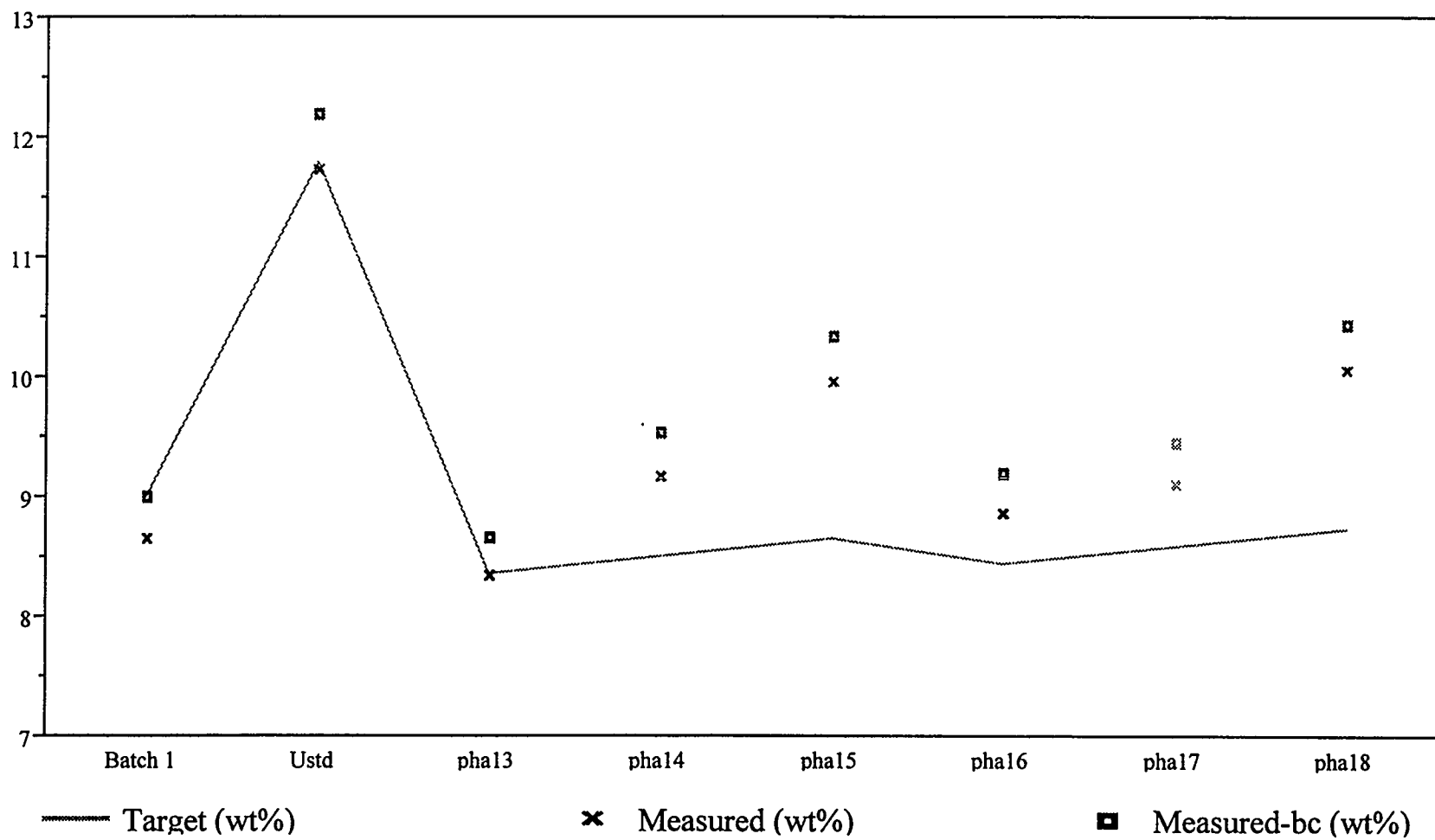


Exhibit A.4: Comparisons of Measurements versus Target Compositions
(concentrations in weight percents)

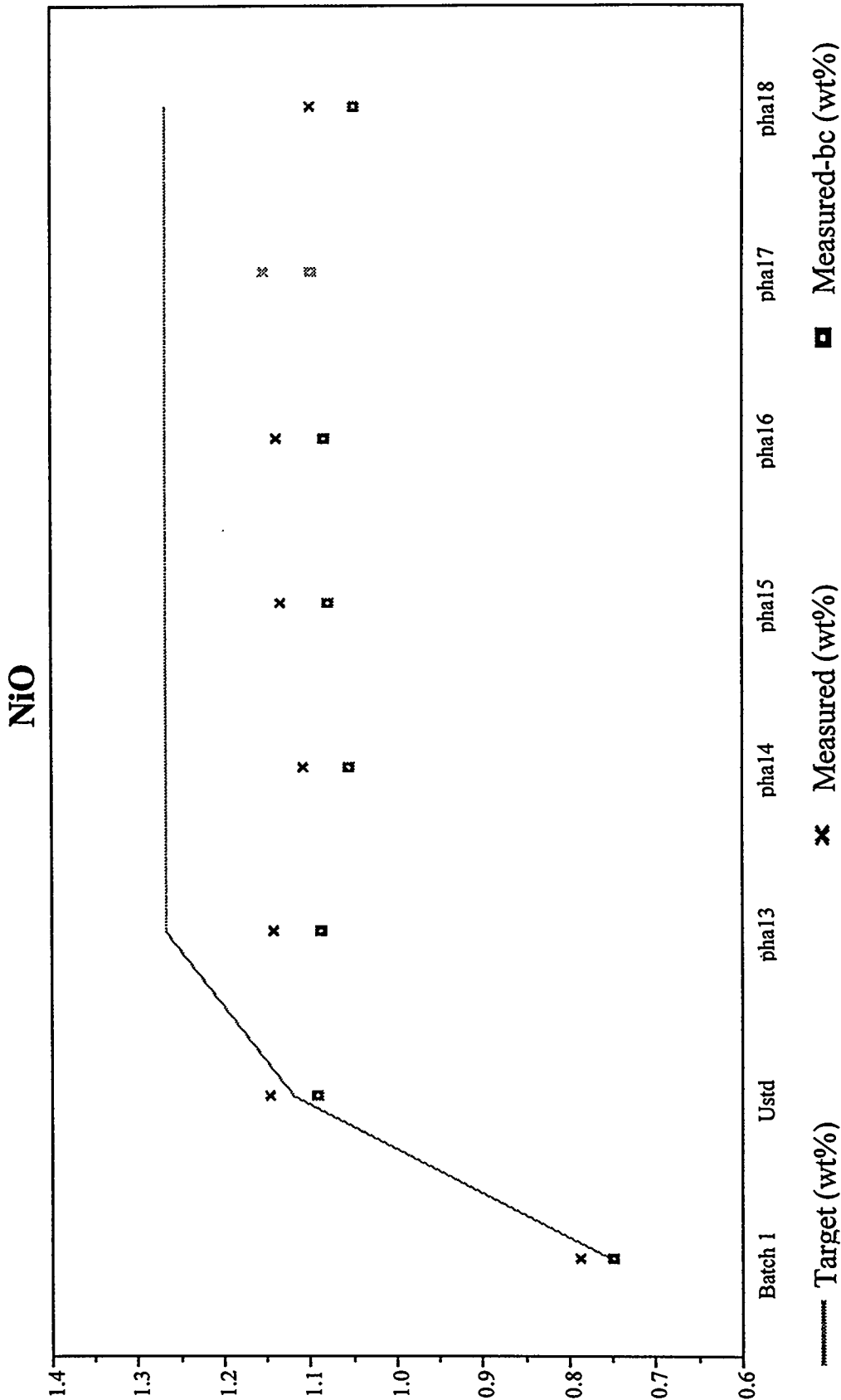


Exhibit A.4: Comparisons of Measurements versus Target Compositions
(concentrations in weight percents)

SiO₂

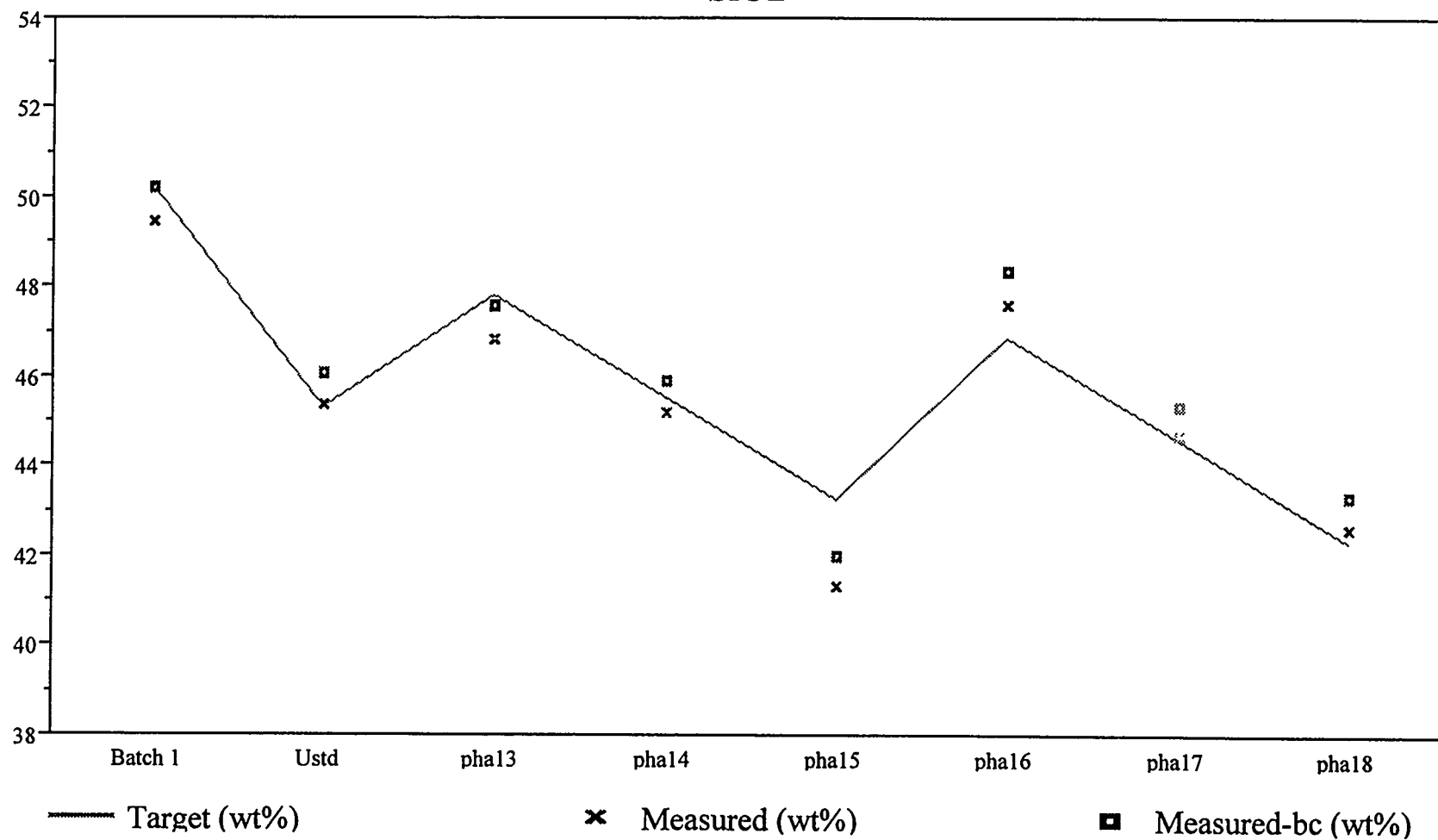


Exhibit A.4: Comparisons of Measurements versus Target Compositions
(concentrations in weight percents)

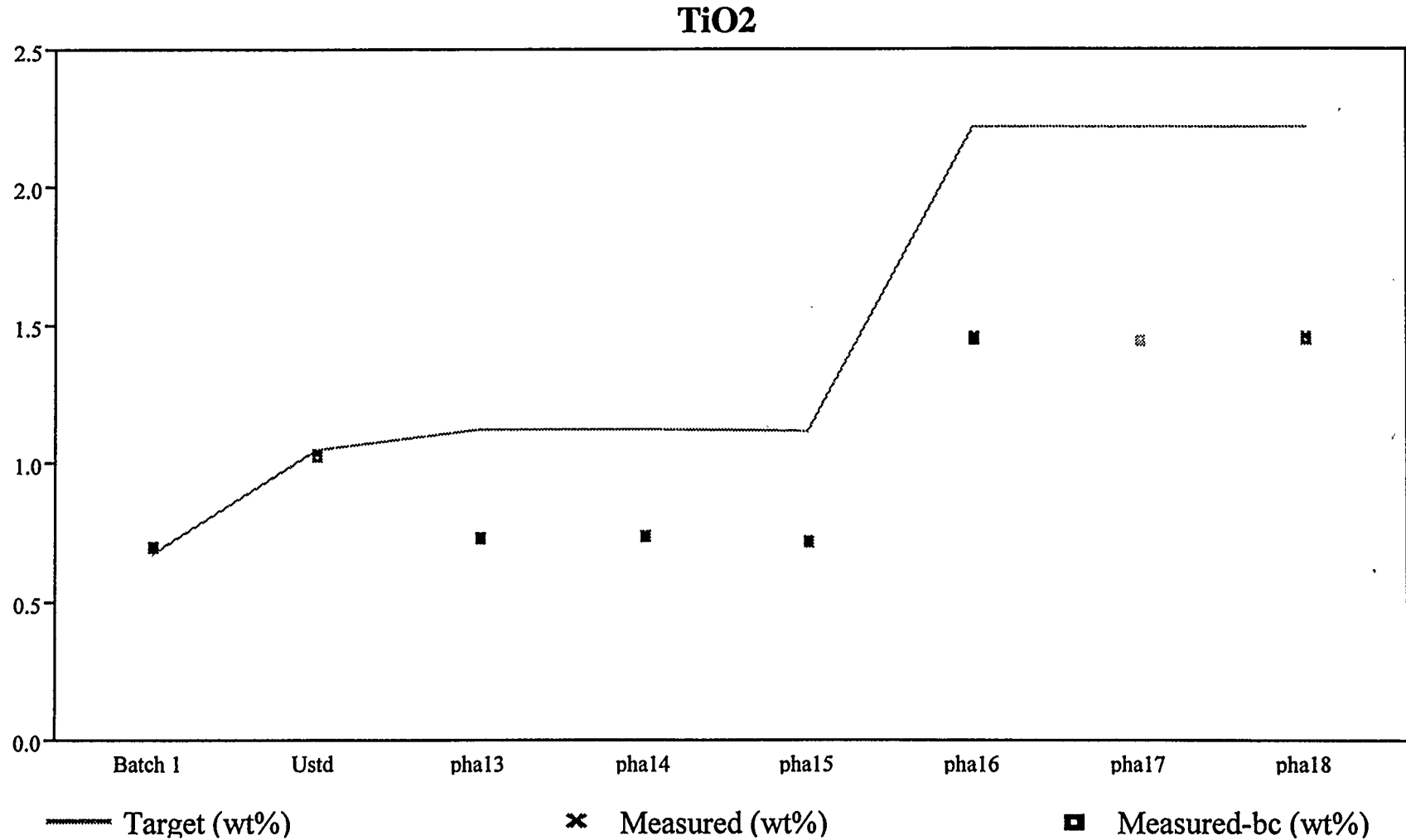


Exhibit A.4: Comparisons of Measurements versus Target Compositions
(concentrations in weight percents)

U3O8

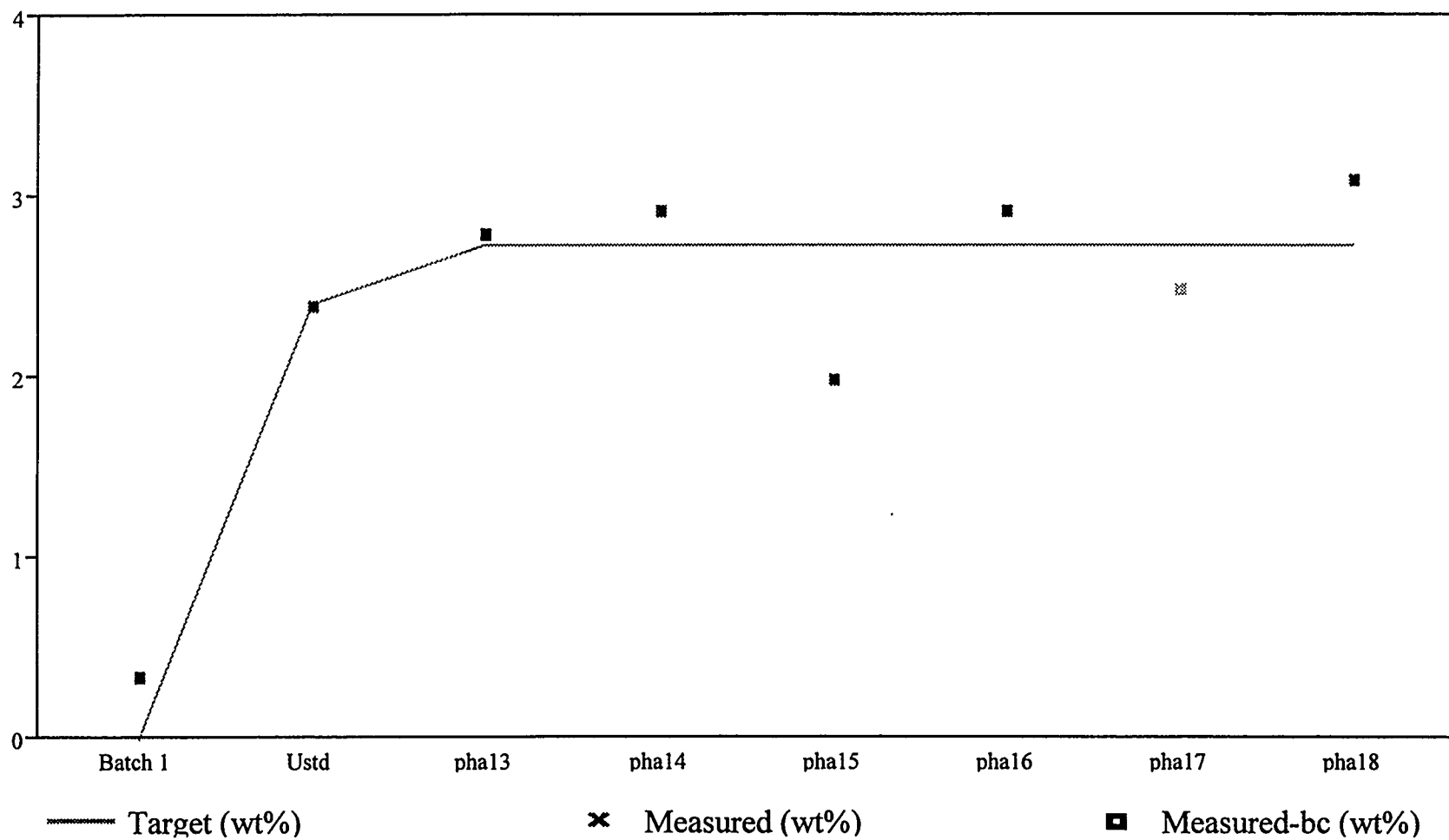


Exhibit A.4: Comparisons of Measurements versus Target Compositions
(concentrations in weight percents)

ZrO₂

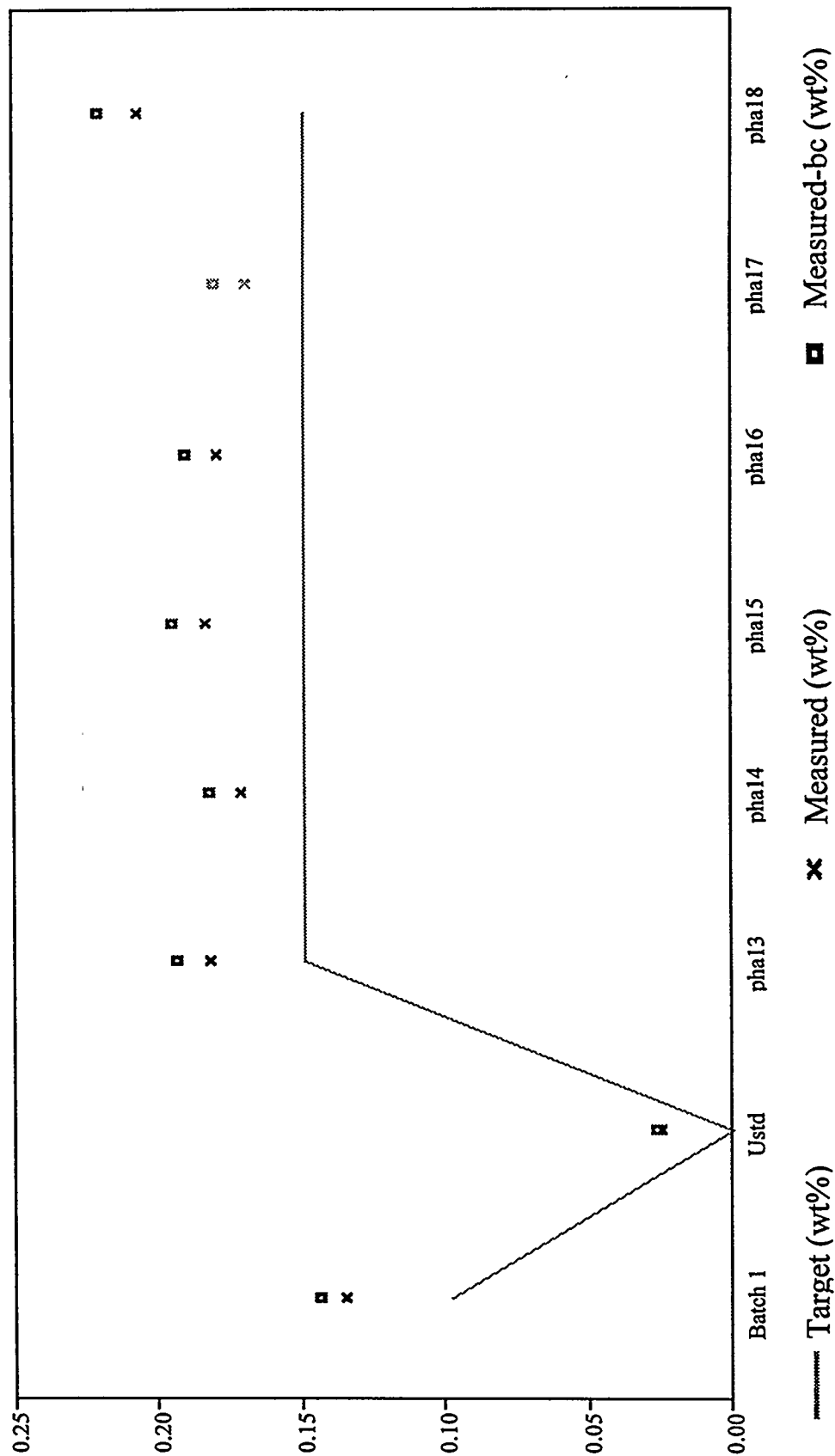


Exhibit A.4: Comparisons of Measurements versus Target Compositions
(concentrations in weight percents)

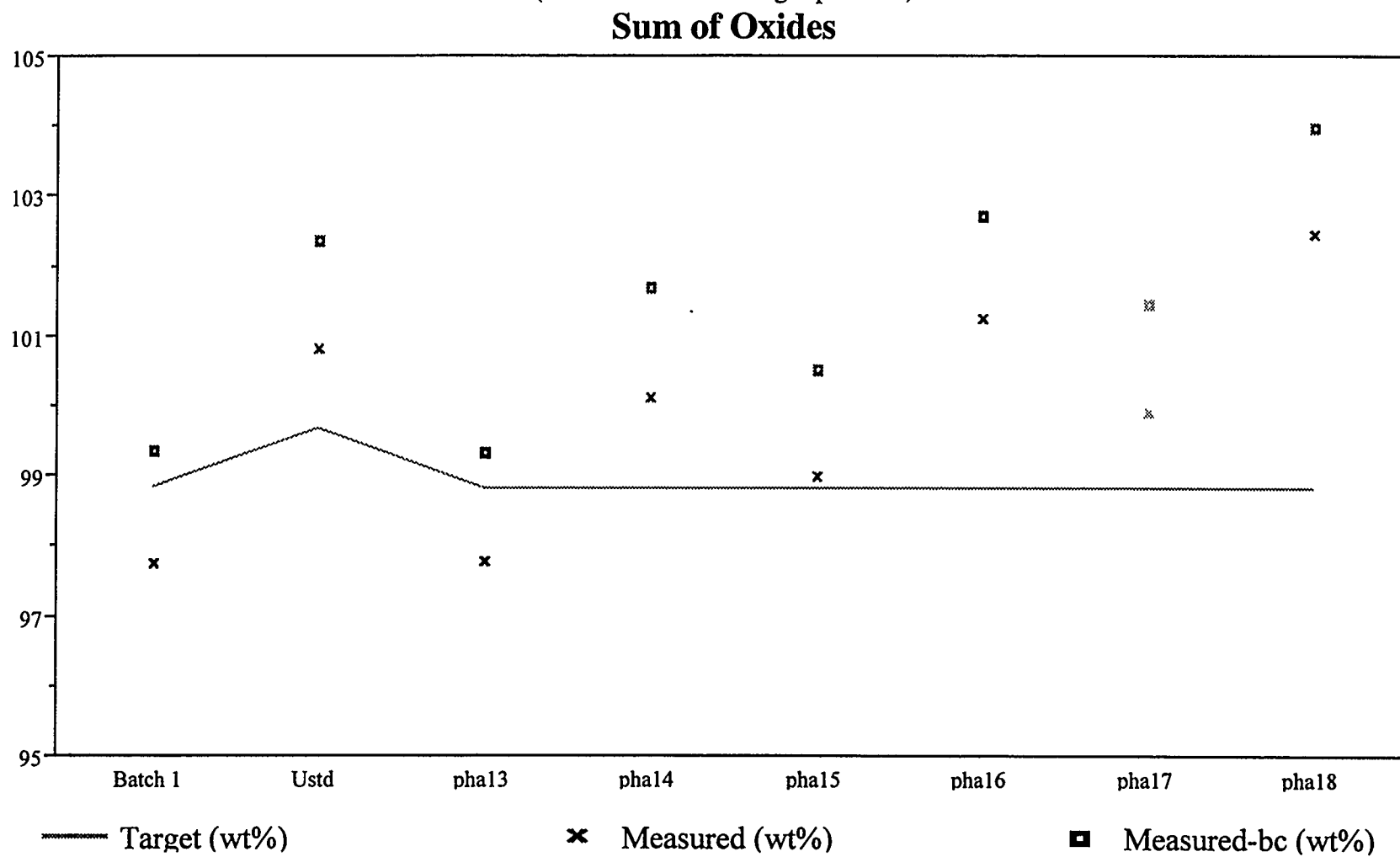
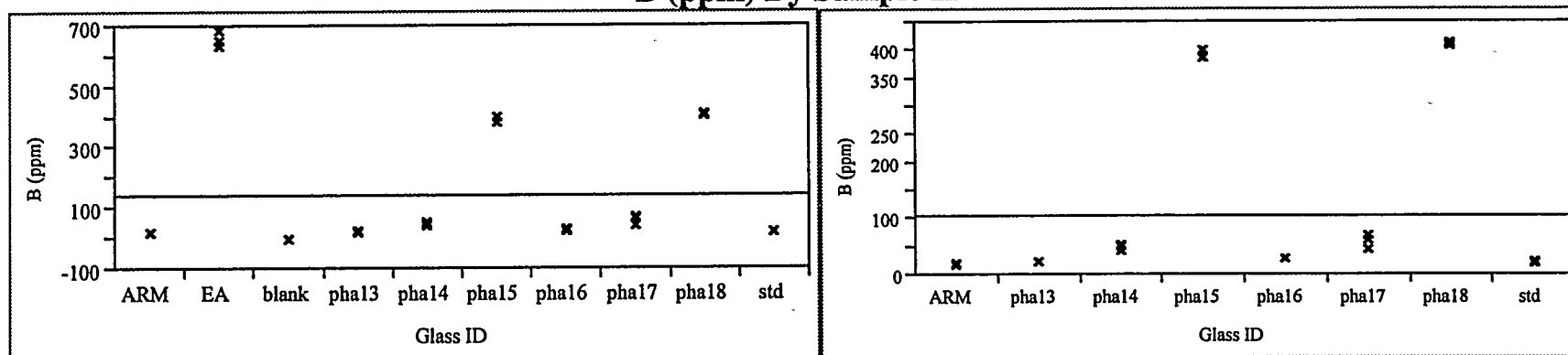


Exhibit A.5: Plots of the Leachate Concentrations by Sample ID by Element

B (ppm) By Sample ID



Si (ppm) By Sample ID

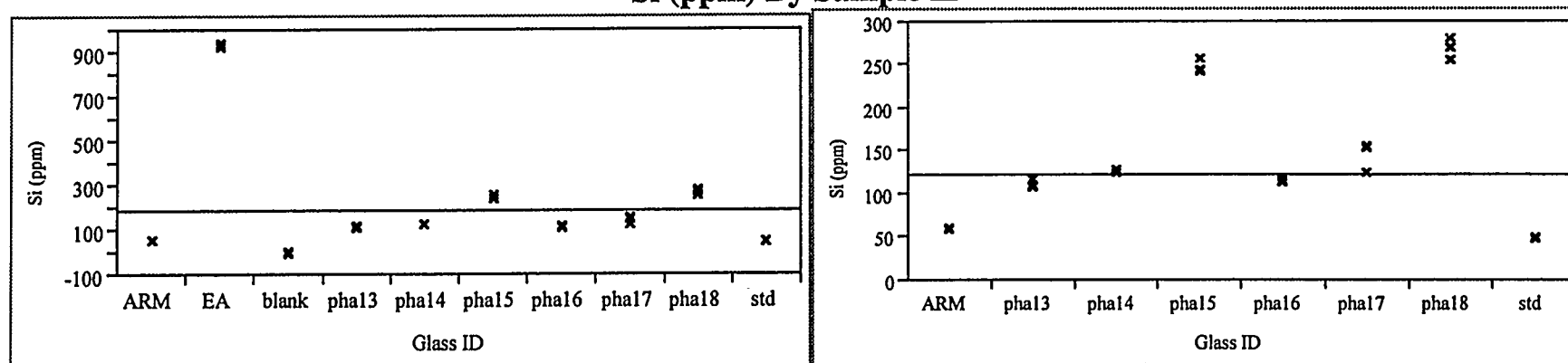
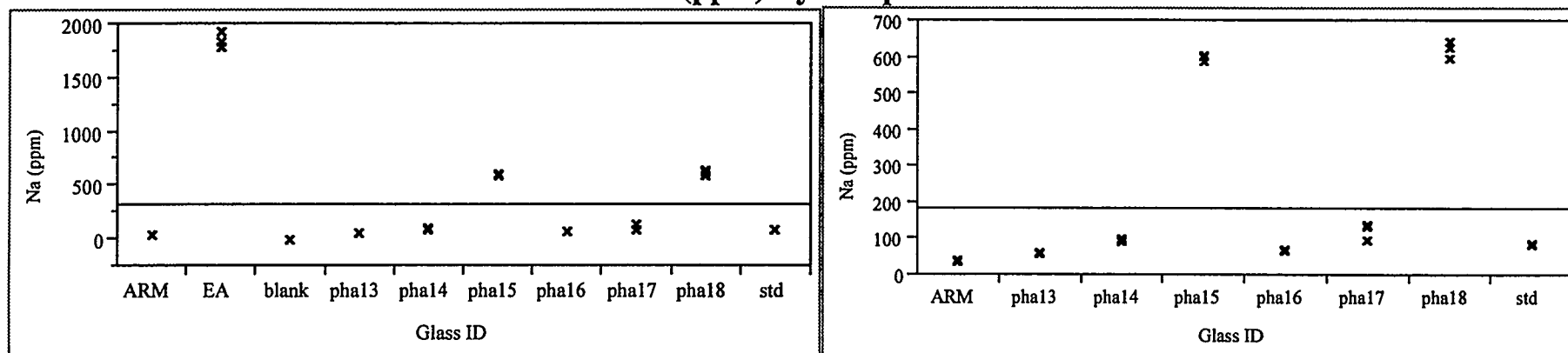


Exhibit A.5: Plots of the Leachate Concentrations by Sample ID by Element
(continued)

Na (ppm) By Sample ID



Li (ppm) By Sample ID

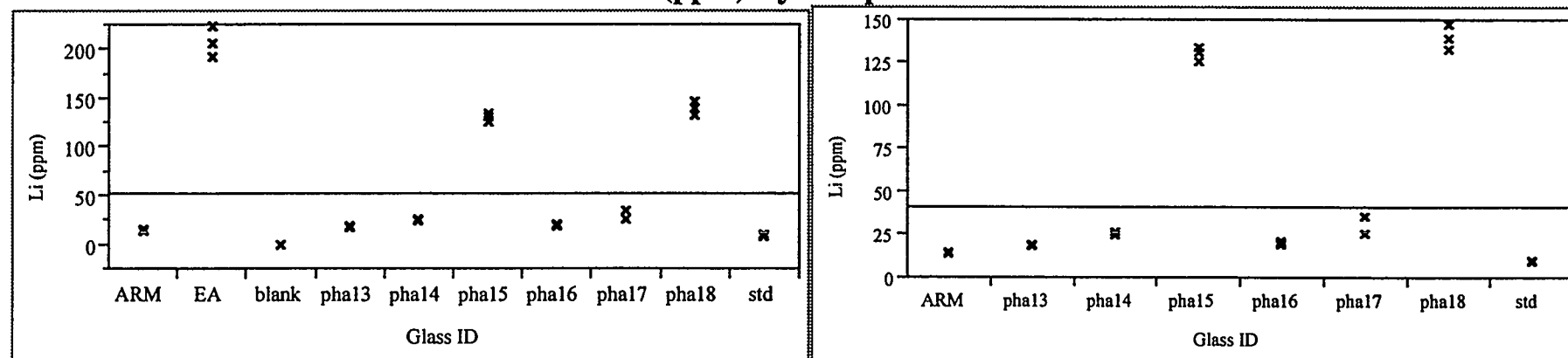


Exhibit A.6: Scatter Plots of the Normalized PCT's

Correlations Using Target Compositions

Variable	log NL[B g/L]	log NL[Si g/L]	log NL[Na g/L]	log NL[Li g/L]
log NL[B g/L]	1.0000	0.9963	0.9993	0.9986
log NL[Si g/L]	0.9963	1.0000	0.9969	0.9984
log NL[Na g/L]	0.9993	0.9969	1.0000	0.9995
log NL[Li g/L]	0.9986	0.9984	0.9995	1.0000

Correlations Using Measured Compositions

Variable	log NL[B g/L]	log NL[Si g/L]	log NL[Na g/L]	log NL[Li g/L]
log NL[B g/L]	1.0000	0.9989	0.9999	0.9998
log NL[Si g/L]	0.9989	1.0000	0.9993	0.9994
log NL[Na g/L]	0.9999	0.9993	1.0000	0.9999
log NL[Li g/L]	0.9998	0.9994	0.9999	1.0000

Correlations Using Bias-Corrected Measured Compositions

Variable	log NL[B g/L]	log NL[Si g/L]	log NL[Na g/L]	log NL[Li g/L]
log NL[B g/L]	1.0000	0.9989	0.9999	0.9998
log NL[Si g/L]	0.9989	1.0000	0.9993	0.9994
log NL[Na g/L]	0.9999	0.9993	1.0000	0.9999
log NL[Li g/L]	0.9998	0.9994	0.9999	1.0000

Scatterplot Matrix

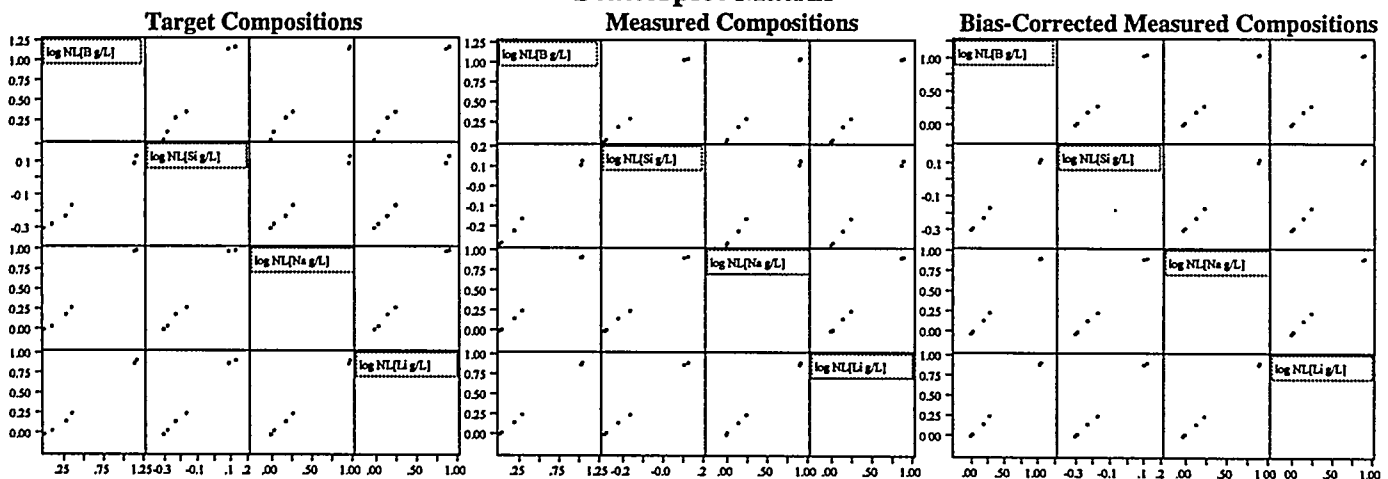
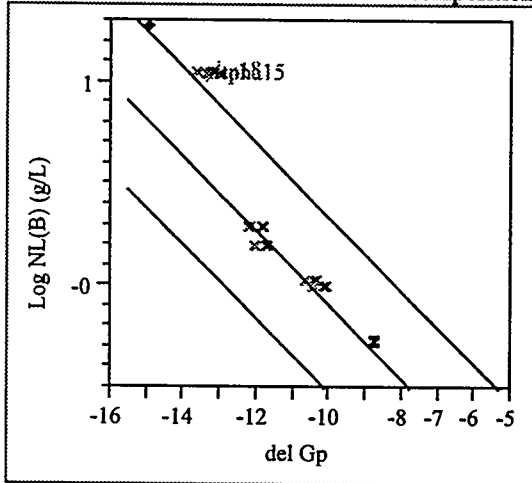
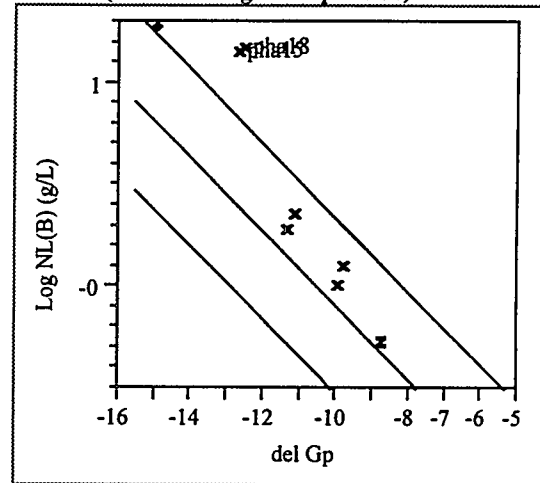


Exhibit A.7: Durability Predictions versus Measured

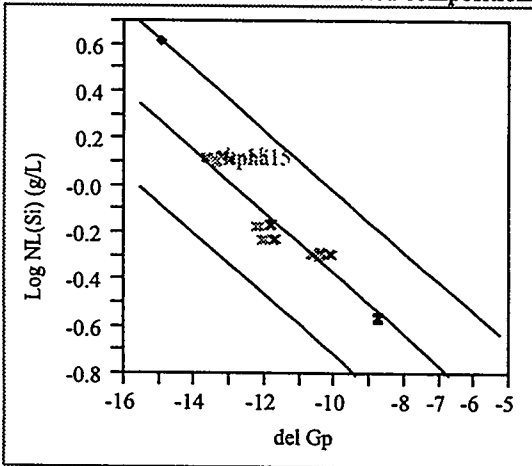
Log NL(B) (g/L) By del Gp(m)
(based on measured and bias-corrected compositions)



Log NL(B) (g/L) By del Gp(m)
(based on target composition)



Log NL(Si) (g/L) By del Gp(m)
(based on measured and bias-corrected compositions)



Log NL(Si) (g/L) By del Gp(m)
(based on target composition)

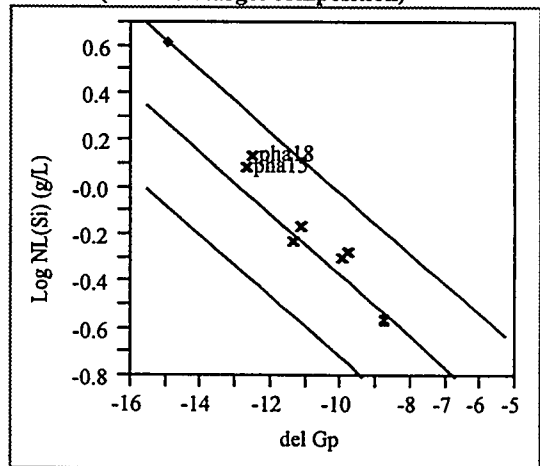
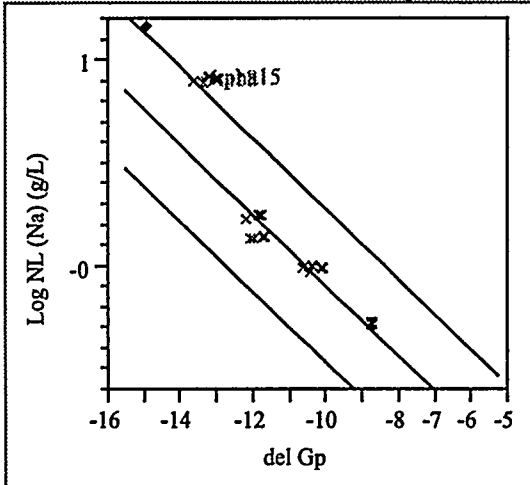
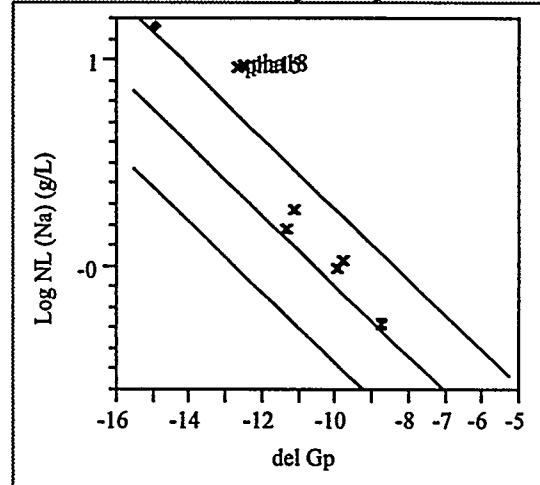


**Exhibit A.7: Durability Predictions versus Measured
(Continued)**

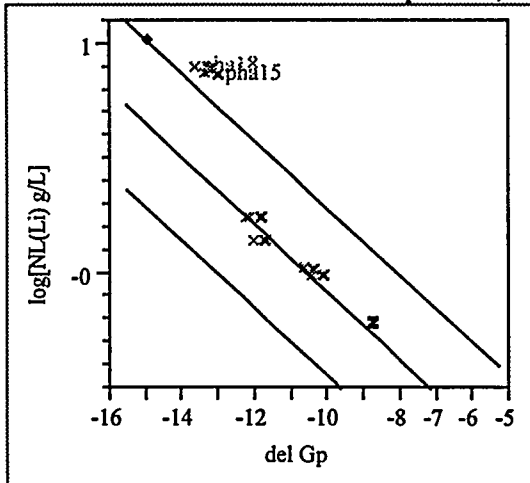
Log NL (Na) (g/L) By del Gp(m)
(based on measured and bias-corrected compositions)



Log NL (Na) (g/L) By del Gp(m)
(based on target composition)



log[NL(Li) g/L] By del Gp(m)
(based on measured and bias-corrected compositions)



log[NL(Li) g/L] By del Gp(m)
(based on target composition)

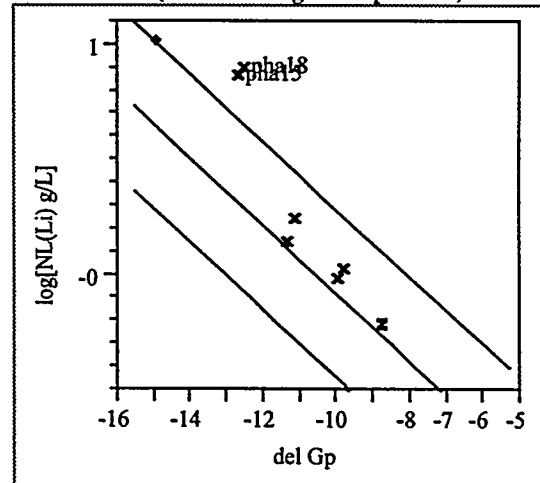
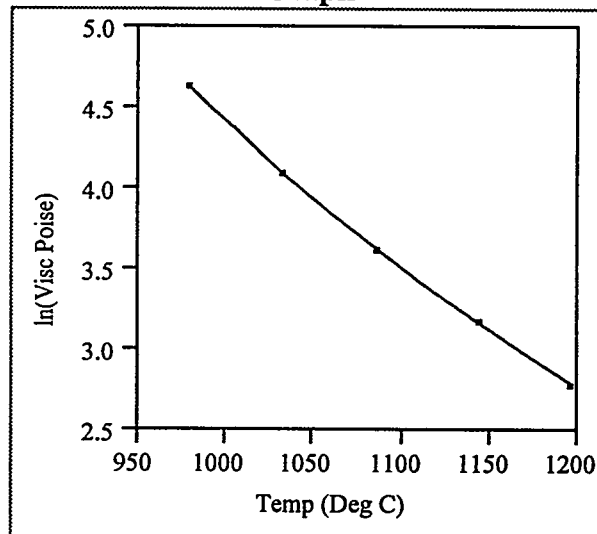


Exhibit A.8: Viscosity Measurements, Fulcher Fits, and Predictions at 1150 °C**pha14**

Parameter	Estimate	ApproxStdErr
A	-4.225485888	0.61254041
B	7308.3964283	1133.34093
C	155.68871194	71.3211669

Graph

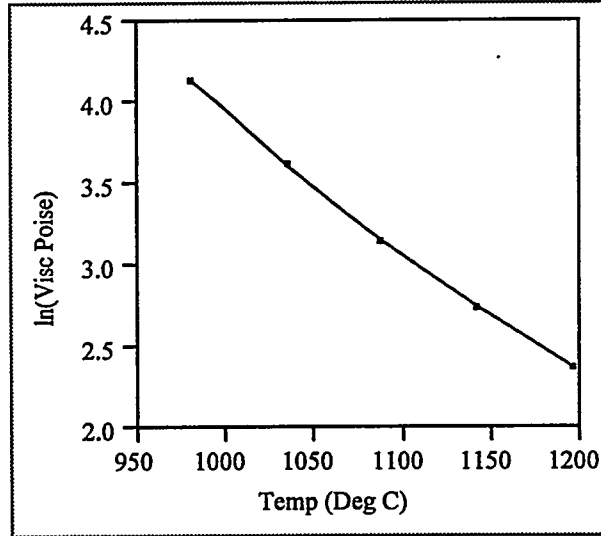
Temp (Deg C)	Visc (Poise)	ln Visc (Fulcher)	ln(Visc Poise)	Visc Pred (Poise)
1197.5	16.21983	2.789601	2.786235	16.27
1144.5	23.89761	3.165607	3.173778	23.70
1086.5	37.32683	3.626155	3.619712	37.57
1033.5	60.43323	4.100218	4.101539	60.35
980	103.637	4.640578	4.640894	103.60
1150	?	3.124724	?	22.75

Exhibit A.8: Viscosity Measurements, Fulcher Fits, and Predictions at 1150 °C
(continued)

pha15

Parameter	Estimate	ApproxStdErr
A	-3.662561525	0.39683813
B	5769.2810675	665.011579
C	242.53958126	47.9658519

Graph



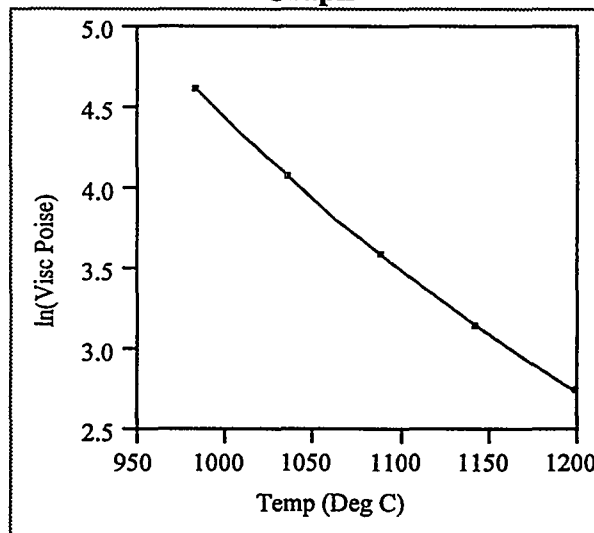
Temp (Deg C)	Visc (Poise)	ln Visc (Fulcher)	ln(Visc Poise)	Visc Pred (Poise)
1197.5	10.81322	2.378821	2.38077	10.79
1142	15.637	2.751596	2.74964	15.67
1088	23.50077	3.161272	3.157033	23.60
1035	37.49484	3.617652	3.624203	37.25
981.5	62.95545	4.144732	4.142427	63.10
1150	?	2.69505	?	14.81

Exhibit A.8: Viscosity Measurements, Fulcher Fits, and Predictions at 1150 °C
(continued)

pha17

Parameter	Estimate	ApproxStdErr
A	-4.145251013	0.62567925
B	6953.2369976	1115.97391
C	190.51181113	71.1436404

Graph



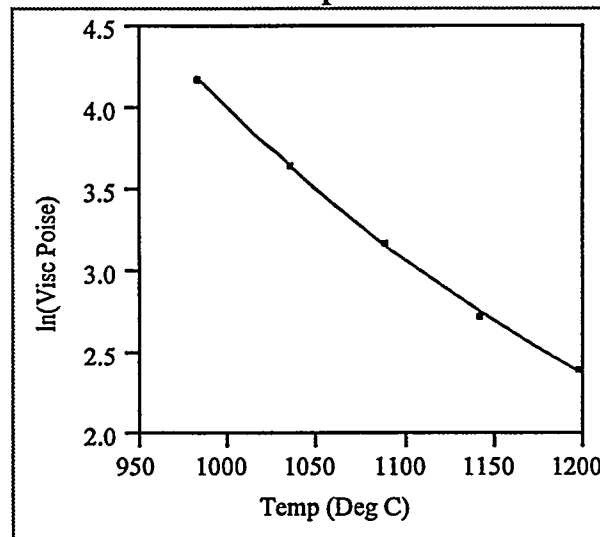
Temp (Deg C)	Visc (Poise)	ln Visc (Fulcher)	ln(Visc Poise)	Visc Pred (Poise)
1199	15.69756	2.749462	2.753505	15.63
1142	23.40302	3.162498	3.152865	23.63
1089.5	36.41017	3.589263	3.594848	36.21
1036	59.14499	4.078681	4.079992	59.07
983	102.2453	4.62868	4.627374	102.38
1150	?	3.101568	?	22.23

Exhibit A.8: Viscosity Measurements, Fulcher Fits, and Predictions at 1150 °C
(continued)

pha18

Parameter	Estimate	ApproxStdErr
A	-3.003211518	1.30132561
B	4628.8729174	1928.78568
C	339.41670781	153.074216

Graph



Temp (Deg C)	Visc (Poise)	ln Visc (Fulcher)	ln(Visc Poise)	Visc Pred (Poise)
1198.5	11.01153	2.384942	2.398943	10.86
1142	15.4271	2.764256	2.736126	15.87
1089	24.02799	3.17205	3.179219	23.86
1036	38.69298	3.641899	3.655658	38.16
983	65.51857	4.189133	4.182334	65.97
1150	?	2.707334	?	14.99

Distribution

J. L. Barnes, 704-3N
N. E. Bibler, 773-A
D. F. Bickford, 773-43A
K. G. Brown, 704-1T
J. T. Carter, 704-3N
J. J. Connelly, 773-41A
A. D. Cozzi, 77-43A
D. A. Crowley, 773-43A
T. B. Edwards, 773-42A
H. H. Elder, 704-S
S. D. Fink, 773-A
J. R. Harbour, 773-43A
E. W. Holtzscheiter, 773-A
R. A. Jacobs, 704-3N
C. M. Jantzen, 773-A
R. T. Jones, 704-3N
D. P. Lambert, 704-1T
L. F. Landon, 704-1T
S. L. Marra, 704-25S
D. B. Moore-Shedrow, 773-A
L. M. Papouchado, 773-A
D. K. Peeler, 773-43A
J. A. Pike, 704-3N
K. J. Rueter, 704-3N
R. F. Schumacher, 773-43A
M. E. Smith, 773-43A
T. K. Snyder, 704-1T
P. C. Suggs, 704-196N
W. L. Tamosaitis, 773-A
R. C. Tuckfield, 773-43A
R. J. Workman, 773-A
TIM (4 copies), 703-43A